Landslide occurrence in East Timor

Sara Soares[1], Claire Mills[1], Mike Sandiford[1] and
Joao dos Reis[2]

Melbourne Energy Institute
Technical paper series

June, 2011

[1]School of Earth Sciences, University of Melbourne

[1]Secretariat of State for Natural Resources, Timor-Leste Government

EXECUTIVE SUMMARY

Background

Mass movements such as landslides and debris flows are important agents of erosion in steep mountains, and are significant landform processes in Timor-Leste. The dominant triggers are earthquakes and high-intensity precipitation events. Timor-Leste is vulnerable to a number of natural hazards, including landslides, with little capacity for response. Seasonal monsoon rains falling on steep slopes cause frequent flash flooding and landslides, which regularly damage and destroy infrastructure, especially in rural areas. Timor-Leste is located in a geological region of high seismic activity and, although historical earthquake activity is relatively limited, earthquakes are expected to be a significant contributor to future landslide hazard.

Geomorphic hazard and risk zonation provides the essential science framework for landslide risk assessment based. Geomorphological studies can provide applied approaches to both mitigation and impact minimisation of natural disasters such as landslides. An essential requirement is the development of an accurate database of active and historical landslides.

Landslide inventory

The findings presented in this report are based on studies undertaken as part of two Masters research projects from the University of Melbourne students, working in conjunction with geologists from the Department of Geology and Mineral Resources within the Secretariat of State for Natural Resources. Field work was conducted from 2010 to 2011 principally in the districts of Ainaro and Baucau. A major outcome of this study is a landslide inventory database showing landslide size distribution for the country mapped using aerial photograph interpretation (API) of one set of detailed aerial photographs acquired in 2001. The inventory includes at 2005 active landslides, ranging in size from .0002 to 1.14 km^2. The largest observed event is located in the suco of Bualale with a width of 1.2 km and an area of 1.14 km^2. The contribution of landslides to the sediment flux shows a clear power law trend over two orders of area magnitude ($\sim 10^2 - 100$ km^2).

The landslide inventory was compared to climate, geology, earthquake and slope maps to distinguish the key controls on landslide distribution. East Timor has been characterised into three broad zones according to the above controls. Zone A is characterised by frequent shallow earthquakes which trigger landslides in steep (>40°) cultivated slopes, and in clay-rich and unconsolidated lithologies in the highlands where annual precipitation exceeds 2000 mm. Zone B is located in the central mountains and is characterised by steep slopes, generally over 40°, where landslides are triggered by high precipitation events on the unstable slopes of cultivated highlands. Zone C landslides are predominantly controlled by geology and climate, rather than steep slopes. Here precipitation can reach 680 mm/month and landslides are clustered in the clay-rich lithologies.

Lacaloi landslide

A field study conducted of a recent landslide in Zone C identified heavy precipitation, lithology and bedrock structure to be the causes of the movement. The landslide is located in the Quelicai sub-district and covered an area of 0.2 km^2. The majority of movement occurred over two days and destroyed rice paddies, houses and gardens. The morphology of the slide shows it to consist of at least three deep-seated rotational blocks with glide planes well into the competent bedrock. Evidence of creep and scarps within regolith layers in the immediate area surrounding the slide indicate that the area is at high risk of further large-scale earth movements.

Future studies

Several recommendations are made with respect to future ongoing landslide hazard:

- Systematic ground-truthing of the landslide database across all of Timor-Leste.

- Monitoring program for ongoing creep and sliding in large active land sliding.

- A survey of incipient landsliding features such as creep scarps are high priority for future survey and planning purposes, in high-risk zones incorporating villages and settlements that are potentially at risk.

- A national framework for incorporating landslide risk assessment in developing key infrastructure such as road and electricity networks, and human settlements.

Table of Contents

ACKNOWLEDGEMENTS

1 Introduction

Timor-Leste is a country very vulnerable to a number of natural hazards, including landslides, with little capacity for response. It is located in an area of high seismic activity and is exposed to earthquakes and tsunamis. Seasonal monsoon rains falling on steep slopes cause frequent flash flooding and landslides, which regularly damage and destroy infrastructure, especially in rural areas. These events cause major disruption to the fragile road network of the country, isolating communities and even districts for days, weeks, or even months. Most contemporary landslides are small, but there is evidence for past massive catastrophic landslides.

Widespread social, infrastructure, health and food vulnerabilities in Timor-Leste are further exacerbated by hazard and climate risks, lack of capacity and weak governance arrangements at the operating level.

Climate change is acknowledged to have the potential to exacerbate all weather-related hazards. Scientific understanding of the nature and incidence of these changes in Timor-Leste remains very limited.

Successful economic development must be based on strong national infrastructure including roads, power, telecommunications, air and sea ports, and urban infrastructure. In Timor-Leste the road network, which is extensive but in poor condition, serves to provide access to rural areas, where the majority of the poor live, and link rural communities to services and participation in the wider society. Roads also sustain important commercial, industrial and service activities in urban areas. The network is vulnerable to erosion and flooding, and access if frequently cut at high risk locations during the wet season.

2 Methods and Approach

The findings presented in this report are part of two Masters research projects from the University of Melbourne focused on Timor's most recent uplift history, of which there has been previous limited research. The projects focused on landscape response to tectonic collision processes, with a specific focus on landsliding processes. Today mass movements occur all over East Timor at different scales, with small landslides abundant. This study seeks to understand the role landslides have played in shaping East Timor's landscape.

Specific aims of the studies are:

- To understand the role of landslides in active mountain belts, in particular their role in shaping East Timor's landscape.

- Quantify the characteristic landslide size distribution responsible for yielding the most amount of sediment.

- Investigate the May 2010 Lacalio landslide in the sub-district of Quelicai.

A regional landslide inventory for East Timor was prepared from aerial photograph interpretation (API) of detailed photographs acquired by the Australian military and Google Earth. The resulting inventory was used in geomorphological statistical analysis. This analysis included characterising the size distribution of landslides and quantifying their contribution to the erosion of the Timor orogen, and an assessment of the dominant triggering mechanism.

Fieldwork was conducted for four weeks in the dry season of 2009, from July 18 – August 14 with the assistance from staff of the DNGRM (Direcção Nacional de Geologia e Recursos Minerais). A second field season in Ainaro and Maubisse from June 25 – July 1, 2010 was marred by intense rainfall and heavy mists that significantly hindered access to river sections. Concurrent fieldwork was also undertaken in the Quelicai sub-district of Baucau, part of which focused on geomorphology mapping of the recent landslide near the village of Lacalio. Mapping was conducted using several base aerial photographs at 1:10,000.
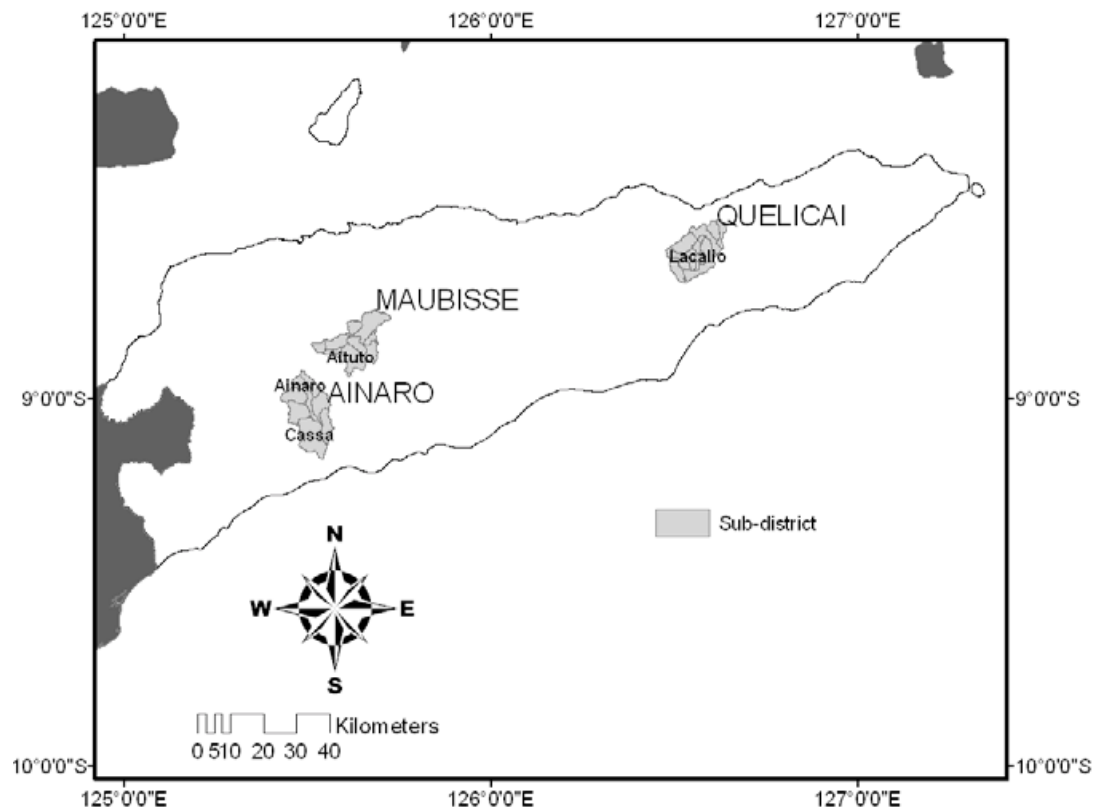
Figure 2.1: Locations of the Ainaro, Maubisse and Quelicai sub-districts. Key sucos of Ainaro, Aituto, Cassa, and Lacalio mentioned in this study are included.

3 Background and Knowledge Status

3.1 Landslides in East Timor mountain belt

Mass movements such as landslides and debris flows are important agents of erosion in steep mountains, and are significant landform processes in Timor-Leste. The dominant triggers are earthquakes and high-intensity precipitation events, thus, the study of the role of landslides in the erosion of young compressional orogens, such as Timor, provides an insight into the dynamic coupling between tectonics, surface erosion processes, and climate.

Mass wasting in the form of bedrock landslides moves material from hillslopes onto the valley floors, where rivers can transport it out of the system. East Timor, therefore, provides a natural laboratory to study landslide processes. From the pervasive presence of recent landslide scars on the set of aerial photographs of Timor-Leste and observations from the two field trips over 2009 to 2010, it is inferred that slope failure is a dominant process in the Timor orogen. Little, however, is known about the contribution to relief destruction and sediment flux at the mountain-belt scale. In this context, this study seeks to investigate whether landslides play a formative role in the evolution of East Timor's landscape.

3.2 Geology of East Timor

The deformation and uplift of the Timor island is the consequence of the Neogene collision between the northern margin of the Australian continental plate with the Banda volcanic arc (Harris et al., 2000; Hall & Wilson, 2000; Audley-Charles, 2004). Located in the centre of the Banda Arc collision zone, Timor comprises a complex fold and thrust belt of Australian continental margin sedimentary lithologies and remnant pre-collisional arc rocks, which became emergent in the last few million years (Haig & McCartain, 2007, Keep & Haig, 2010) (Figure 3.1).

Audley-Charles (1968) was the first to produce a lithostratigraphic synthesis of the exposed rocks of East Timor, which have recently been simplified by Haig et al. (2007) into five main tectono-stratigraphic units (Figure 3.2 and 3.3).

The Permian to middle Jurassic Gondwana Megasequence comprises intracratonic basin sediments deposited in north-eastern Gondwana. Late Jurassic to Neogene deposition of the Australian Margin Megasequence followed the break-up of Gondwana and subsidence at ~155 Ma. Recently, detailed biostratigraphic studies by researchers from the University of Western Australia (UWA) have revealed Late Permian, Late Triassic and Early Jurassic ages for strata of the Gondwana Megasequence (McCartain et al., 2006; Haig et al., 2007).

Onset of collision in the mid to late Neogene produced the Synorogenic Melange, formed at least partly through diapirism. Also known as the Bobonaro Scaly Clay, it was interpreted by Audley-Charles (1968) and subsequent workers (e.g. Carter et al., 1976) as an olistromal gravity slide deposit that moved from north to south in response to the southward tilting of Timor.
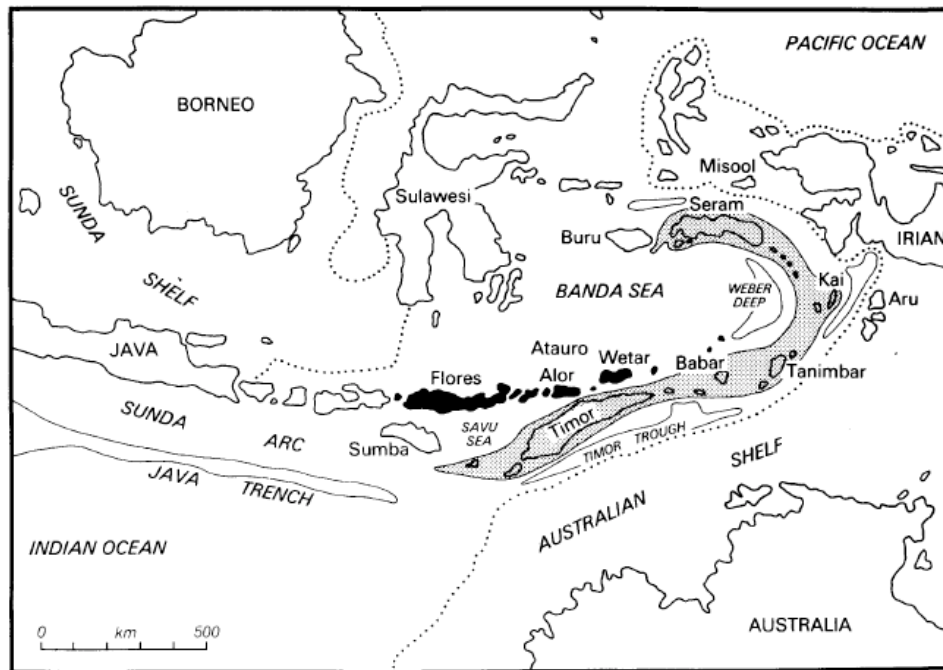
Figure 3.1: Taken from Audley-Charles, 1986, showing the dark volcanic Inner Banda Arc, and the crosshatched Outer Banda Arc comprising mostly of deformed sedimentary units from the Australian margin.
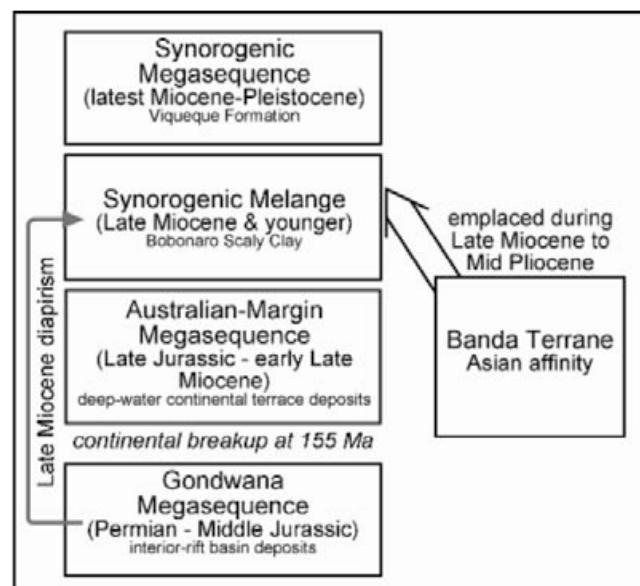

Figure 3.2: Tectonostratigraphic summary of the exposed lithologies in East Timor taken from Haig et al., (2007).
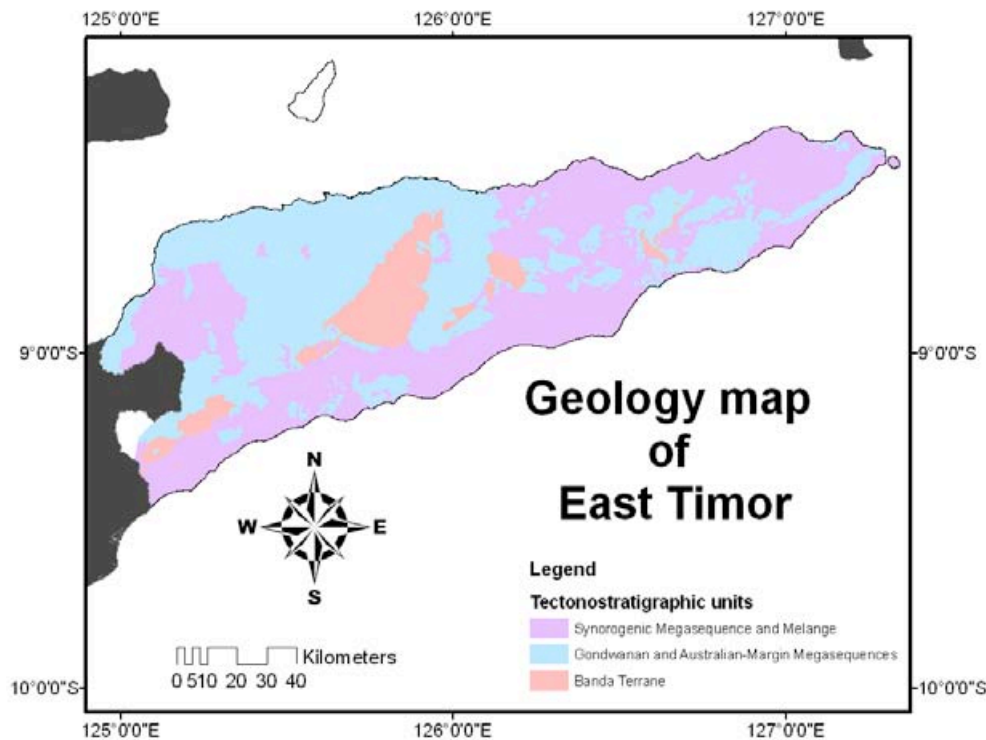
Figure 3.3: Geology map of East Timor showing the distribution of the main tectonostratigraphic elements. Adapted from Audley-Charles (1968) using tectonostratigraphic framework of Haig et al., (2007).

The Banda Terrane of probable Asian affinity was also progressively emplaced onto the Australian continental margin as a series of thrust sheets following the Late Neogene collision.

Post-collisional uplift and the emergence of present-day Timor are associated with the deposition of the relatively undeformed Synorogenic Megasequence. These comprise sedimentary packages of the Viqueque Formation, the raised limestone reefs of the Baucau Limestone, and the uplifted river terraces of the Ainaro Gravels (Audley-Charles, 1968).

3.3 Climate and topography

The erosion of mountain belts controls their topographic and structural evolution and is the main source of sediment delivered to oceans (Dadson et al., 2003). Dramatic topography is a feature of Timor, which at just over 70 km wide, has many peaks over 2500 mASL and reaches a maximum height of 2963 mASL in the central Ramelau Range. Topography exerts a strong influence on the climate, controlling variations in both temperature and rainfall. Winds from cold high-pressure areas over Australia travelling from the south-east accumulate moisture as they cross the Timor Sea and bring reliable rain to the areas south of the Ramelau Range. The northern coast is in the rain shadow and as a result is predominantly dry in contrast to the moist southern portion and mountainous central region of the country (Monk et al., 1997). Compare Ainaro located south of the Ramelau Range in the foothills at an altitude of approximately 800 mASL and receives annual rainfall of 1800 mm, to the capital Dili

6

located in the north and receives approximately 800 mm (Durand, 2006 p.38). East Timor is predominately influenced by the monsoon climate, which is characterised by very little seasonal variation in temperature, and frequent torrential rains. For example, in the capital city Dili maximum daily rainfall has been recorded at 275 mm, which is nearly 30% of the annual mean rainfall (Sandlund et al., 2001). Rainfall in East Timor (Figure 3.4) can be divided into two distinct patterns: the Northern Monomodal Rainfall Pattern, affecting the northern side of the country and producing a 4 to 6 month wet season beginning in December; and the Southern Bimodal Rainfall Pattern, which affects the southern portion of the country, and consists of a longer wet season, lasting 7 to 9 months, with rainfall peaking in December and May (Keefer, 2000).

The rainfall patterns of East Timor are significantly influenced by the Southern Oscillation and 'El Nino' weather patterns, which can produce severe droughts as well as flooding (Keefer, 2000). In Ainaro, the annual rainfall is up to 50% less than average in El Nino years. El Nino suppresses rainfall in the January to March wet season, with some places in East Timor experiencing only 25% of the rainfall usually received in these months. Mountainous areas, characterised by very steep terrain at altitudes above 600 m, can experience temperatures below 24 ºC, rainfall above 1500 mm and a dry season that lasts four months (Sandlund et al., 2001).
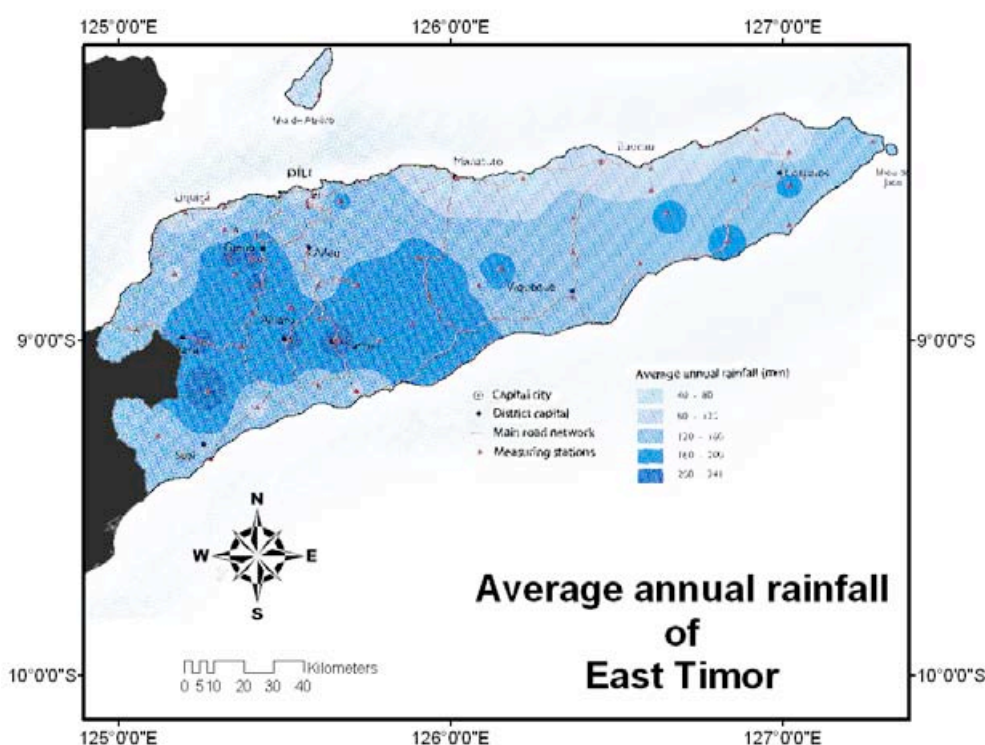
Figure 3.4: Average annual rainfall map for East Timor, taken from LIDEL.

Monthly mean temperatures vary by no more than 3˚C between the coolest months of July and August to the warmest months of October and November (Keefer, 2000), and vary with altitude (Figure 3.5). Dili, which at sea level, has a mean annual temperature of 27.5 ºC, in contrast to Maubisse, which, at over 1400 m ASL, has only a mean monthly temperature of 19.8 ºC (Keefer, 2000). Maximum, minimum and

7
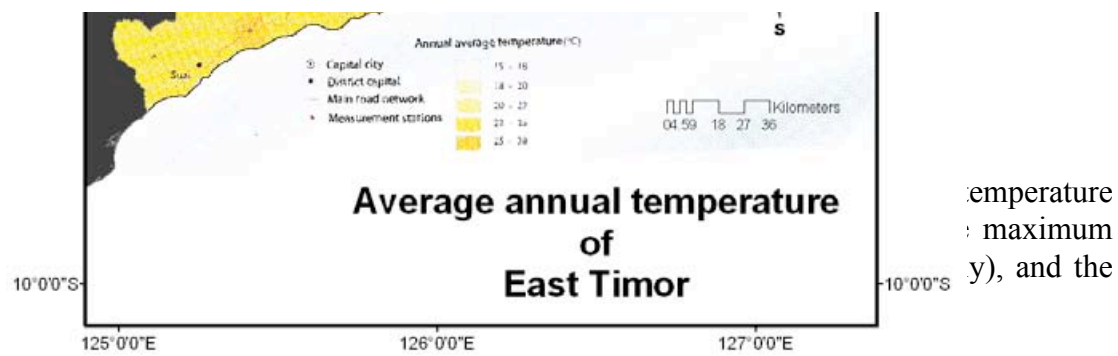
Figure 3.5: Average annual temperature map for East Timor, taken from LIDEL.

3.4 Earthquakes

Situated at the centre of the Banda Arc collision zone, East Timor is located in an area of high seismic activity and is exposed to earthquakes and tsunamis. Strong earthquakes of magnitudes greater than 6 in Indonesia have been felt in Timor. Tremors from a 6.9-magnitude earthquake that struck off Indonesia's Sulawesi island on August 2009 were felt in the capital Dili. A massive earthquake striking off Indonesia's Sumatra triggered the December 2004 tsunami that killed more than 230,000 people in a dozen countries.

East Timor itself experiences shallow earthquakes (Figure 3.6), which can cause significant damage to infrastructure. In areas with unstable slopes these earthquakes can trigger landslides, which impact on peoples' lives, roads, infrastructure, livestock and property.

Figure 3.6: Earthquake epicentres in the East Timor region using ANSS dataset.

8

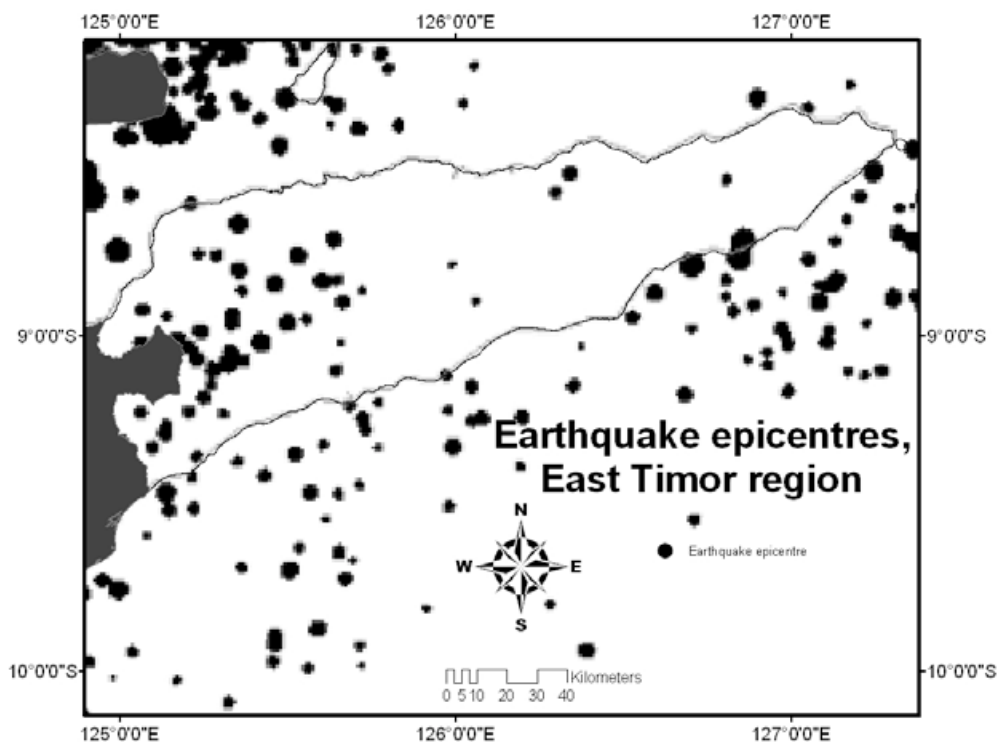There are currently no seismic hazard maps nor is there an earthquake-monitoring network available in Timor-Leste. The Badang Meteorolic Geophysica in Jakarta and Japan provide earthquakes measurements and seismic data.

3.5 Natural Hazards Issues and Priorities

Countries in the Asia-Pacific region experience some of the world's worst natural disasters – frequent earthquakes, volcanic eruptions, cyclones and annual monsoons – and there is abundant evidence that natural disasters disproportionately affect developing countries.

Following the increasing recognition that disasters erode hard-won development gains, international policymakers have focused on disaster risk reduction as a key priority. The Hyogo Framework for Action 2005-2015 is the key instrument for implementing disaster risk reduction, adopted by the Member States of the United Nations. Its overarching goal is to build the resilience of nations and communities to disasters, by achieving substantive reduction of disaster losses by 2015 – in lives, and in the social, economic, and environmental assets of communities and countries. It lists the following 5 key priority areas for action:

1. Ensure that disaster risk reduction in a national and a local priority with a strong institutional basis for implementation;

2. Identify, assess, and monitor disaster risks – and enhance early warning;

3. Use knowledge, innovation, and education to build a culture of safety and resilience at all levels;

4. Reduce the underlying risk factors;

5. Strengthen disaster preparedness for effective response at all levels.

3.5.1 Key Government Institutions

The broad responsibility for various aspects of vulnerability and risk assessments is spread across the Ministry of Social Solidarity and the Ministry for Economy and Development. Countrywide response is centrally managed through the National Disaster Management Directorate (NDMD) of the Ministry of Social Solidarity, which suffers from a chronic lack of human and financial resources, irregular access to information and data due to the lack of adequate systems and equipment, and is overburdened with frequent occurrences. The impacts of disasters are also further exacerbated by slow, centralised response (World Bank, 2010).

The National Disaster Management Directorate (NDMD):

The NDMD is responsible to the Secretary of State for Social Assistance and National Disasters, and is the focal point for management of the overall response to catastrophic events. It is within the Ministry of Social Solidarity.

The National Directorate for Environmental Services (NDES):

The NDES, and the associated National Directorate for International Environment Affairs, are responsible for climate change adaptation and mitigation matters. It is within the Ministry of Economy and Development.

3.5.2 Natural Hazards Policies and Priorities

The commitments of the Government of Timor-Leste towards disaster risk management are embedded in the IV Constitutional Government Program of the Council of Ministers for 2007-2012, where it identifies the following essential priorities to be addressed:

- Identification of risk zones;

- Creation of early warning systems particularly relating to rains and droughts;

- Development of human resource capacity in the area of disaster risk management;

- Ability to provide immediate response when disasters occur;

- Establish inter-sectoral coordination mechanisms to respond to natural disaster.

In 2008, the Government of Timor-Leste adopted the National Disaster Risk Management (NDRM) Policy and is fulfilling its commitments to the United Nations Framework Convention on Climate Change by submitting the Initial National Communication, as well as developing a National Adaptation Program for Action (World Bank, 2010).

The Secretary of State for Natural Disasters and Social Assistance has identified the following needs for assistance in implementing the NDRM Policy (World Bank, 2010):

- Technical assistance support for development of the DRM institutional framework and legislation.

- Technical assistance support for DRM planning across government sectors and, associated, technical assistance for vulnerability assessment.

- Technical assistance support for hazard monitoring, data management and mapping.

- Professional development of staff in areas of hazards, vulnerability assessment and organisational management for DRM.

- Support for the development of district and subdistrict structures and capacity for DRM.

4 Landslides in East Timor

4.1 Landslide inventory for East Timor

In order to investigate how landslides contribute to the erosion of East Timor today, a regional landslide inventory was prepared (Figure 4.1). The inventory provides information regarding past occurrences of landslides in East Timor and a summary of the characteristic landslide size distribution responsible for yielding the most sediment. The main predisposing factors for landsliding in East Timor are high-intensity precipitation in combination with upland farming practices and deforestation. Soil erosion caused by clearing of vegetation on steep slopes is a major environmental problem in East Timor, leading to increase runoff rate and volume (Sandlund et al., 2001).

All landslide scars and debris flow characteristics identified were mapped using the ESRI® ArcMap™ 9.3 software from:

- Aerial photograph interpretation (API) of detailed aerial photographs acquired by the Australian military from 2001;

- SRTM 90 m digital elevation model with shaded relief;

- 2005 topographic maps with a 40 m contour interval.

Landslide mapping via API is a convenient and efficient way to appraise landslide occurrence in steep terrain with difficult access. The landslides identified in this study are defined by the total area disturbed and includes both the scar area and deposition zone. The landslides were mapped on the basis of characteristic landforms, and the confidence of interpretation is based on the distinctness of those landforms. Landslide activity is a relative expression of geomorphic youthfulness, which is highly dependent upon the local geologic and climatic environment. With time, these distinctions grow more subtle as erosion removes or covers these landforms until they resemble those produced by geologic processes and conditions unrelated to landsliding. Landslides disrupt the vegetation cover and stand out as highly reflective areas in light-absorbing surroundings. Recent landslides can be discerned on aerial photographs using morphometric criteria, including arcuate shape of the slope failure, exposure of bedrock in the scar, and deposition of coarse debris downslope. Reflectivity contrasts between vegetated and non-vegetated zones fade as erosion scars are colonized by secondary growth, thus adding a distinction between recent and sub-recent events. While small scars disappear entirely once they become overgrown, larger failures remain visible by the upward projection of their geometric characteristics through the second-growth vegetation. Large and fully overgrown failures were detected using DEM derived shaded relief images and Google Earth. Coalescing or superimposed landslides were mapped separately where possible. Factors affecting landslide interpretation as a result of air photo quality include scale, vintage, sun angle, vegetation, cloud cover, and other characteristics. East Timor is heavily vegetated with forested terrain, and as such, there is room for significant error and underestimates (see Brardinoni et al., 2003 for discussion).
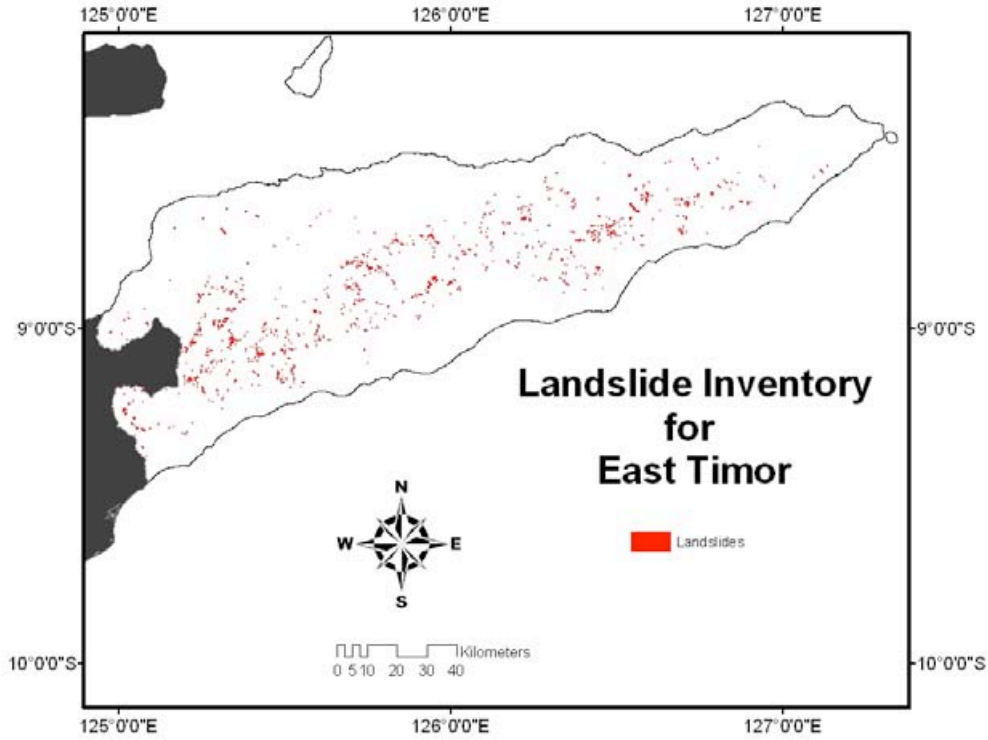
11

Figure 4.1: Landslide inventory of 2005 landslides for East Timor compiled during this study.

A total of 2005 landslides were mapped using these methods in East Timor focusing on the central mountainous region where slopes generally exceed 40 degrees. The data obtained in this study is considered to be of regional reconnaissance scale and quality. The 2005 landslides analyzed in East Timor shows that landslide area ranges over two orders of magnitude (Figure 4.2), for magnitudes greater than 2.5×10^{-2} km^2. The largest observed event from this inventory has a width of 1.2 km and an area of 1.14 km^2. The geometry of the mapped landslides are approximately elliptical with an aspect ratio of about 3. A majority of the landslides were mapped in unconsolidated recent lithologies of the Synorogenic Megasequence and the clay-rich Synorogenic Melange, and have long runout distances.

Hovius et al.'s study (1997) demonstrated that landslides exhibit a magnitude-frequency distribution that may be written in a cumulative form:

$$n_c(A \geq A_c) = \kappa (A_c / A_r)^{-\beta} A_r \qquad (1)$$

when $n_c(A \geq A_c)$ is the number of slides per year of magnitude greater than or equal to A_c over a reference area A_r, κ is the rate of landsliding per unit area per year, and β is a dimensionless scaling exponent. A_r is defined as 1 km^2, and the best fit power law model is obtained by linear regression. This trend is also typically observed in magnitude-frequency relationships for landslides (e.g. Hovius et al., 1997; Malamud et al., 2004).

The distribution of landslides in East Timor was investigated using this method, plotting the number of landslides mapped in the inventory against their areas on a log-log histogram. The results were plotted on logarithmic axes in order to discern

underlying regularity in the distribution of slide number by area, employing logarithmic bin widths ($\log_{10}w = 0.0782921$), as in most inventory programmes only a part of the distribution will be detected. This distribution displays a very clear negative power-law relation spanning two orders of magnitude (Figure 4.2). The plot of the number of landslides equal or greater than the smallest landslide area, employing logarithmic bin widths ($\log_{10}w = 0.0782921$), also has a power law relationship with a gradient of approximately -1 (Figure 4.3). Independent studies from other regions suggest that power-law magnitude frequency distribution and scale invariance is a general property of landsliding (e.g. Hovius et al., 1997; Brardinoni and Church, 2004; Malamud et al., 2004). This is whether one defines landslide magnitude by scar area (Hovius et al., 1997, 2000), or by volume (Hungr et al., 1999; Dai and Lee, 2001) or by total area disturbed including the deposition zone (Pelletier et al., 1997; Guzzetti et al., 2002; this study).

In this study, $A_r = 1$ km^2, and the best fit power law model was obtained by linear regression over the data range from 2.5×10^{-2} km^2 to 1.14×10^{0} km^2. The lower bound of reliable landslide number estimates is at 2.5×10^{-2} km^2.

The geometry of the mapped landslides are approximately elliptical with an aspect ratio of about 3. A majority of the landslides were mapped in unconsolidated recent lithologies of the Synorogenic Megasequence and the clay-rich Synorogenic Melange, and have long runout distances. The relationship between the landslide area and short axis of a best fit bounding rectangle was plotted on a logarithmic axes (Figure 4.6). The short axis (width) is shown to be roughly equal to the square root of the landslide area.
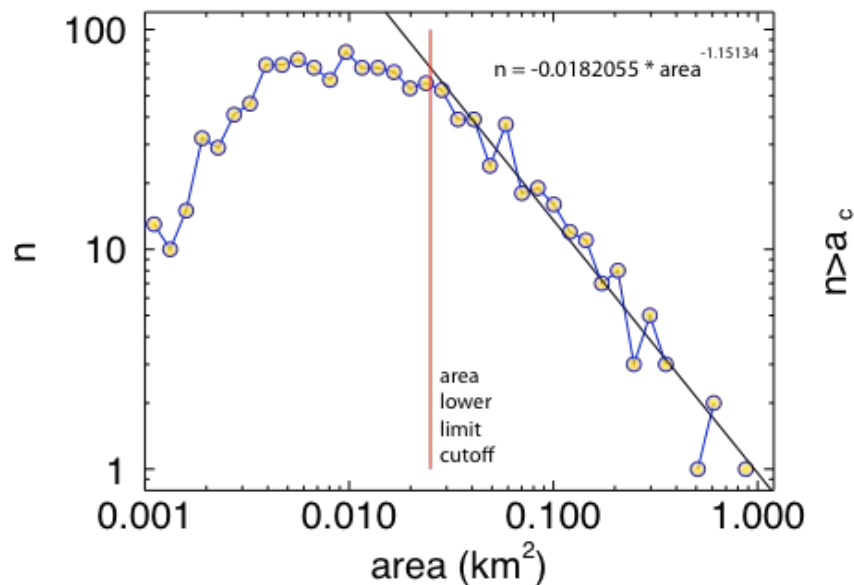

Figure 4.2: Power law relation between the number and magnitude of landslides in East Timor, where n_{TOTAL} = 2005 employing logarithmic bin widths ($\log_{10}w$ = 0.0782921). Mapping method puts lower bound landslide number estimates at about 2.5×10^{-2} km^{-2}. Above this cutoff, a very clear power law trend is observable. Best fit straight line over this trend yields a gradient of -1.15134, which is equal to the exponent β in the following equation $n_c(A{\geq}A_c) = \varkappa(A_c / A_r)^{-\beta}A_r$ (1). Kink in the upper end values of the histogram may be a mapping artifact or reflection of size discontinuity in mass wasting mechanics.
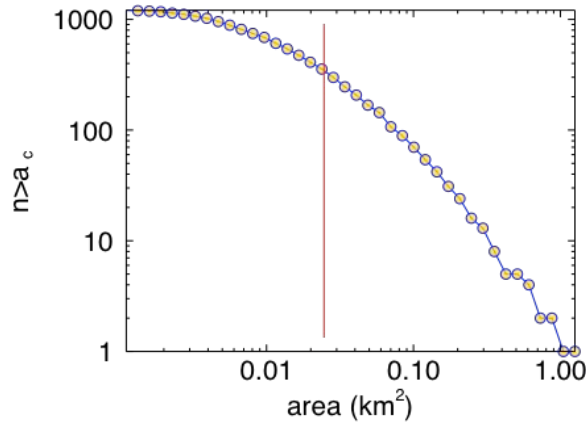
13

Figure 4.3: Number of landslides equal to or greater than landslide area employing logarithmic bin widths ($\log_{10}w = 0.0782921$) also has a power law relationship with a gradient of approximately -1.
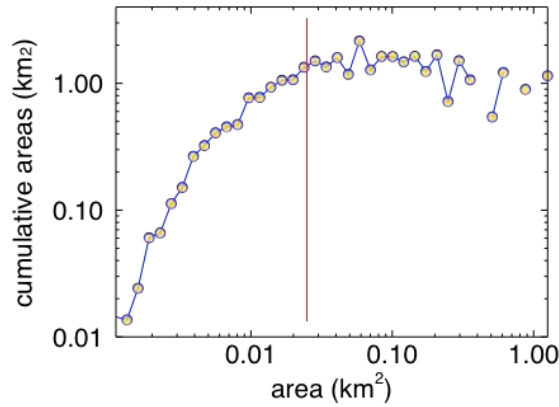
Figure 4.4: Relation between the cumulative areas and landslide area employing logarithmic bin widths of ($\log_{10}w = 0.0782921$), showing the lower bound cut-off at 2.5×10^{-2} km^{-2}. The plot illustrates that the cumulative areas of the many small landslides above the cut-off are of equal magnitude to the contribution of the few upper scale ones.

Figure 4.5: Power law exponent (β) illustrating the change of the exponent - the 'roll-over' effect – for areas below the lower-limit cut-off at 2.5×10^{-2} km^2.

14

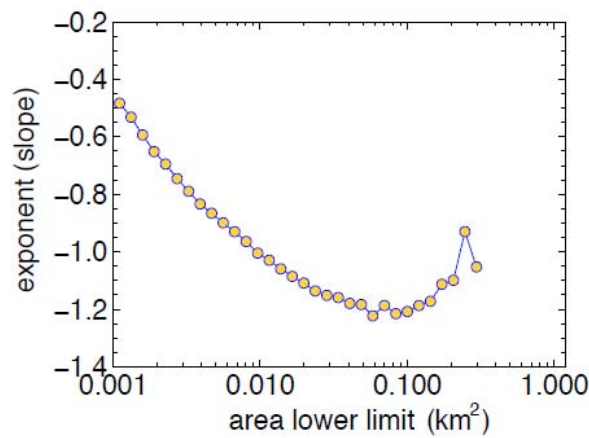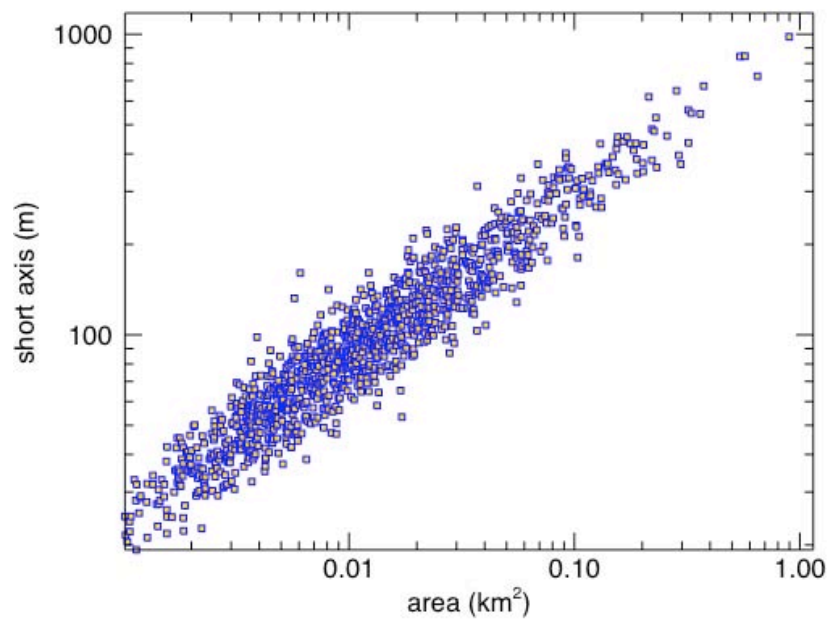**Figure 4.6:** Relationship between landslide area and short axis of bounding rectangle (width of the landslide).

The amount of both small and large deposits completely eroded since the emplacement of the oldest landslide in the sample is unknown. However, previous work in similar topography in East Taiwan (Hovius et al., 2000) has demonstrated that small landslide scars and deposits remain visible on remote sensed imagery for approximately 10 years before revegetation precludes systematic detection. Guthrie and Evans (2007) have shown from frequency magnitude analysis combined with extinctions and appearances of landside features over time that temporal persistence is a function of landslide area indicating, for example, that landslides of 1 km^2 in area would persist for 25 years while a rockslide of 2.7 km^2 in area would persist for 8000 years. Several highly reflective landslides from the aerial photographs were visited in the 2010 field season (Figure 4.7). Most were reactivated by the recent wet season, but one of the highly reflective slides near the hamlet Cassa had since been revegetated and would now not be visible on an aerial photo. Reactivation of multiple or successive failures at the same site are difficult to represent in, and interpret from, the landslide inventory.

4.2 Landslide geomorphology

In the Baucau-Viqueque area where precipitation can reach 680 mm/month, landslides and debris flows are widespread (Figure 4.8). Here landslides are seen to occur in the friable and unconsolidated lithologies of the Synorogenic Megasequence, mapped by Audley-Charles (1968) as the Viqueque formation. The tectonic Synorogenic Melange (formerly the "Bobonaro Scaly Clay") is most susceptible to landslides. These formations are composed of shaly and chaotic melanges, and have a high clay content which readily swells in the presence of water (Rodrigues et al., 2003). In the Bobonaro district, long, low-angle slopes of 10° separated by steeper, more dissected terrain of the intervening slopes provide a characteristic landform

15

signature (Figure 4.9). Intense and prolonged precipitation plays a major role as both triggering new failures and in the reactivation of landslide bodies.

These landforms and lithological controls on landslide susceptiblity are comparable to the *calanchi* of central of Italy (Figure 4.10). The calanchi are a distinct denudation landform of central Italy, where the high gradient of the slope and the low permeability of the lithotypes comprise to reduce infiltration of water favouring rapid surface streamflow, with the consequent cutting of dense drainage networks.

The largest mapped landslide in the inventory is located in the hamlet of Bualale on the night of 16 March, 2000 (Figure 4.11). More than 250 people (50 families) were affected, and the landslide destroyed the only road and bridge to the nearby village of Lassorolai. The distance from the main scarp to the toe of the landslide is 4,330 m. Initial failure occurred in sandstones and clays of the Synorogenic Megasequence and Melange. Lateral slides occurred as the major landslide moved down slope. These slides are still active. Comparison between the aerial photo taken in 2001, a year after the intial failure, with the recent 2010 Google Earth© image shows a five-fold increase in the affected area and a significant full flowing stream developed (Figure 4.12).

Prior to the intial event, a small ephemeral stream occupied this area. This situation is comparable to the recent landslide in Aituto which was also triggered by prolonged intense rainfall during the recent wet season in June, 2010 (Figure 4.13). Less than a month after the event, a concentration of surface runoff over the landslide surface (Figure 4.13B) indicated the initiation of a steady flowing stream. However, unlike the Bualalae landslide, local residents reported that prior to the Aituto event there was no stream (they had to walk long distances to collect water). These two recent large magnitude (> 1 km^2) examples provide insight into the initiaton and expansion of a catchment through landsliding. Large deep seated events such as these generate concave shaped head scarps that concentrate runoff and cause incision of not only the landslide deposit but also headward erosion of the landslide scarp.

In East Timor, many valley-head landslide scars are arcuate and form semicircular clusters which appear to fan out from a common branching point (Figure 4.14). Headwaters consist of large amphitheater-shaped concavities. A large downward concavity on the northern flank of the Cablac mountain range with an area of 0.9 km^2 is interpreted to have formed by a landslide (Figure 4.15 A).

16

B

A

Figure 4.7: A Several deep-seated landslides in Cassa exposing white planktonic foraminiferal marls, 2001 aerial photo. **B** Visit to the site during the 2010 field season.
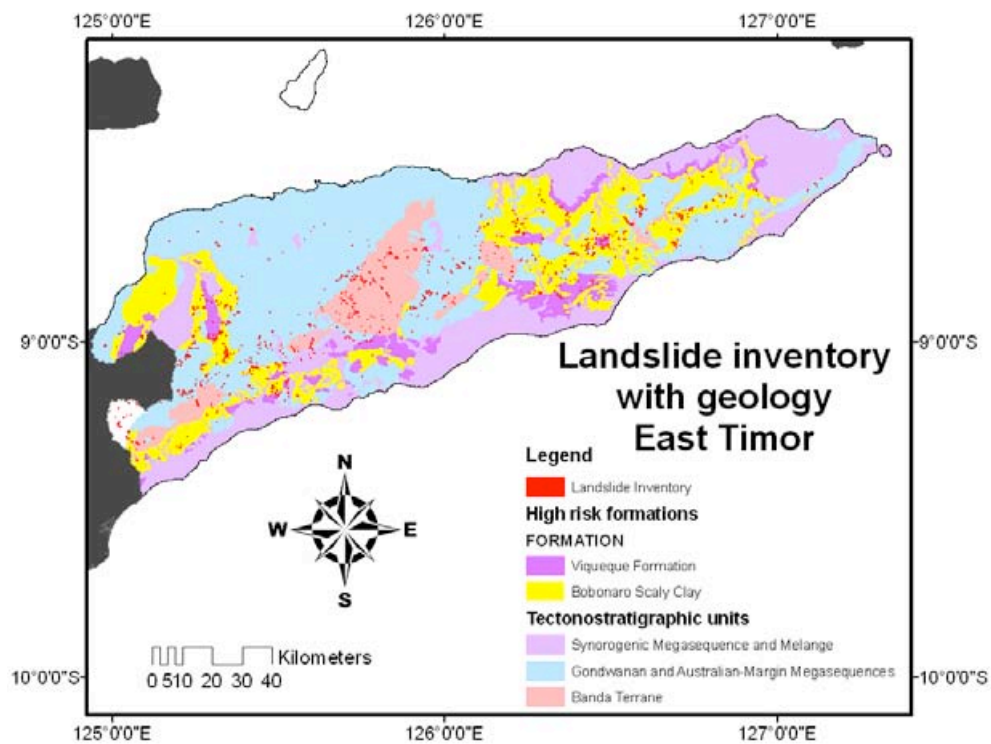

Figure 4.8: Landslide inventory with geology. Landslides are prevalent in areas with friable and unconsolidated lithologies of the Viqueque formation of the Synorogenic Megasequence, and the Synorogenic Melange ('Bobonaro Scaly Clay').

17

D

B
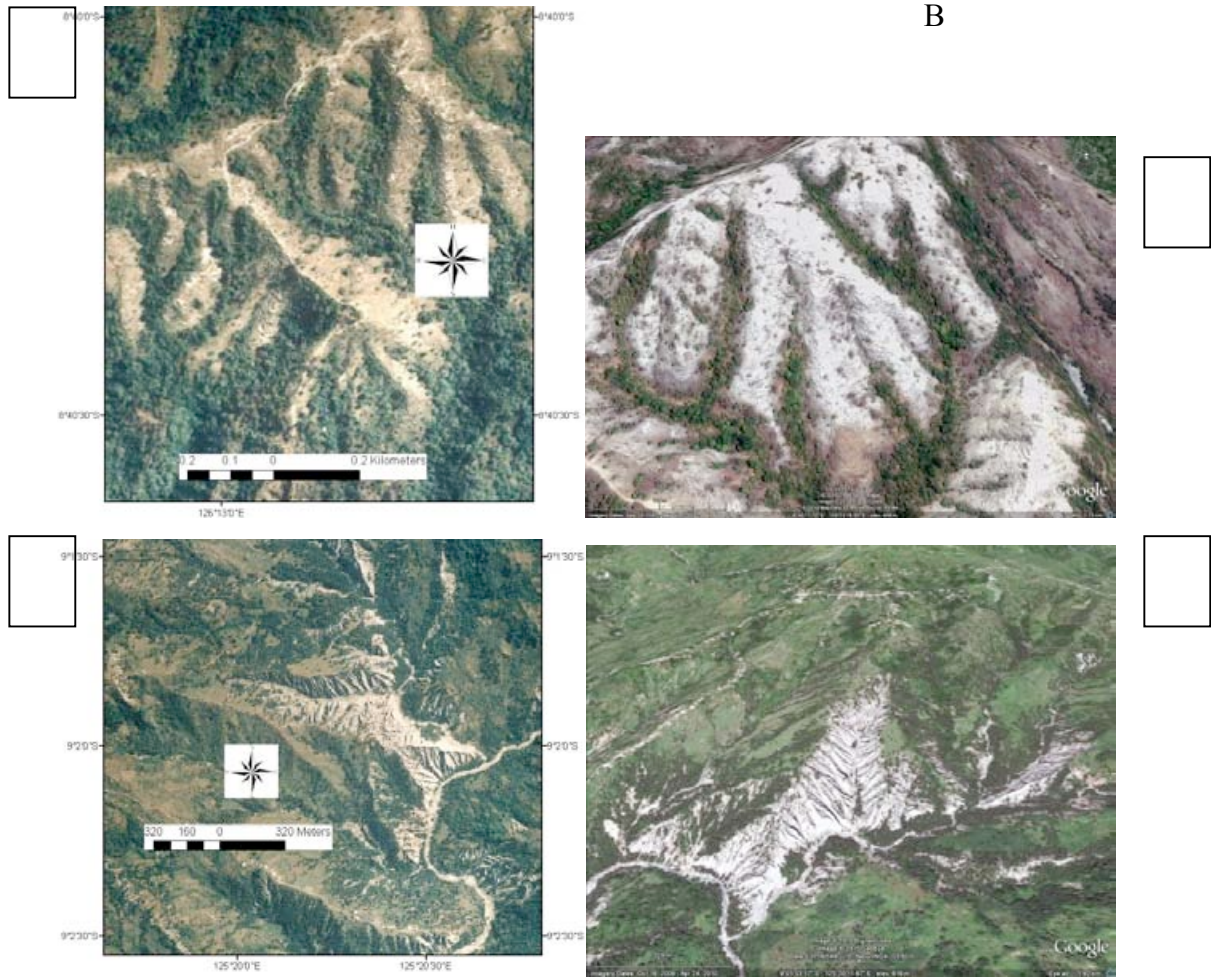
Figure 4.9: Distinct denudation landform of the Synorogenic Melange (Bobonaro Scaly Clay). A 2001 Aerial photo and B Google Earth© image of denuded hillslopes with parallel pattern type network developed showing distinct soil creep. C 2001 aerial photo and D 2010 Google Earth© image, Bobonaro district. The slopes are denuded and the clays of the hillslope are dissected by a dense network of inclined to steeply inclined rills and V-shaped gullies, separated by narrow, sharp crested interfluves.

Figure 4.10: Examples of *calanchi* basin with **A** dendritic and **B** parallel pattern drainage network. These denudation landforms Taken from Buccolini & Coco (2010).

.

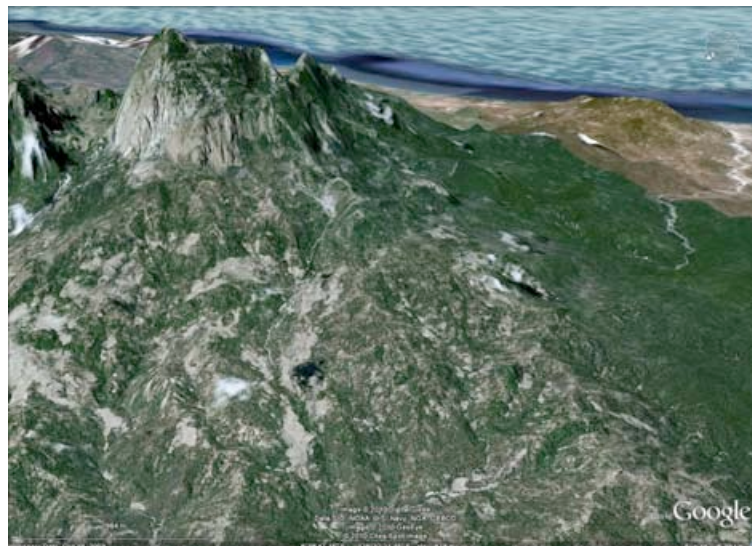**Figure 4.11:** 2010 Google Earth © image of Bualale landslide looking south-east.

A   B   B
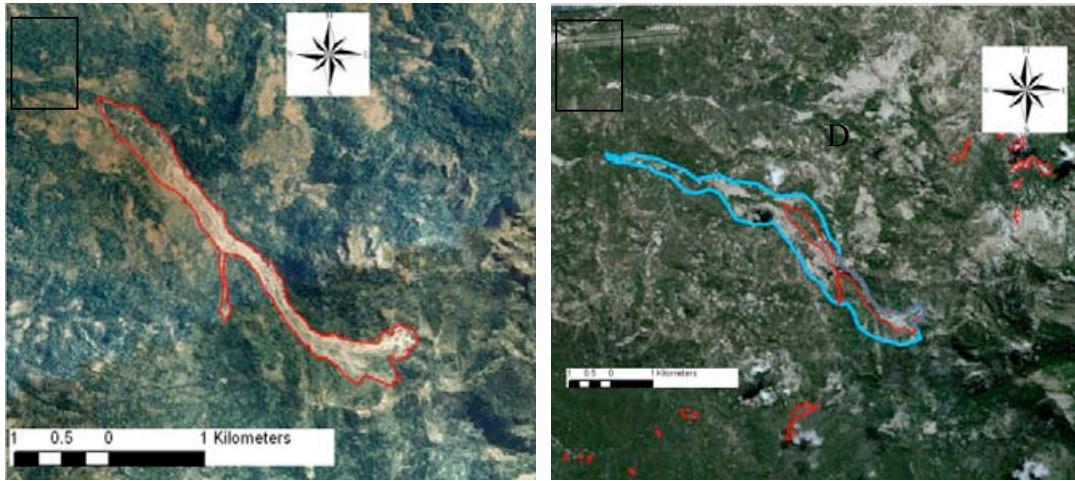
Figure 4.12: Change in extent of affected landslide area from 1.146 km² in the 2001 aerial photograph **A**, to 5.496 km² in the 2010 Google Earth© image **B** .

Figure 4.13: Landslide in the hamlet of Aituto which occurred in June during the wet season after three consecutive days of intense rainfall. **A** Landslide deposit comprising of angular siltstone and calcilutites boulders and gravels. **B** Surface runoff flowing over the landslide deposit. **C** The landslide scarp is located on the south side of the Aituto Anticline, with the accumulation zone diverging into two distinct flow tracks. **D** Walking up the western flow track of the landslide.

Figure 4.14: A Deep-seated landslide with arcuate landslide scarp in the Banda Terrane (Lolotoi formation Audley-Charles, 1968) Manatuto district. **B** Circular deep-seated scarps in the Banda Terrane, Manufahi district.
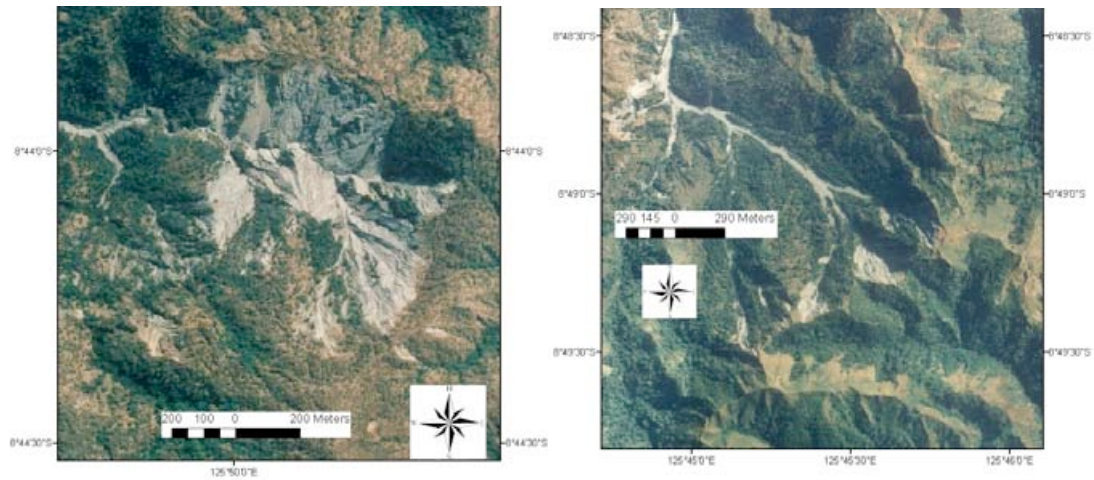

Figure 4.15: A Downward concave morphology of a landslide headscarp on the north facing flank of the Cablac mountain range. **B** The amphitheatre shaped headwaters of the 'Ainaro collapse' north of Ainaro villa, whose geometrical evolution is a result of landsliding.

Mount Buisaralao in Ainaro is an excellent example summarising catchment expansion via landsliding (Figure 4.16). A large landslide from this hillslope deposited a large amount of debris on top of one of the older 'Ainaro collapse' debris terraces and initiated the Sigé river, which has incised both the landslide scar and deposit forming steep debris bound terraces. Stream entrenchment of the Sigé river has promoted valley-floor lowering through the landslide debris and into bedrock, exposing bedded silstones and sandstones.

21

C

E

Figure 4.16: A Contributing landsliding mass from Mount Buisaralao is outpacing the ability of the Sigé river to remove the material. **B** Alluvium of Sigé river comprising bioturbated siltstones. **C** and **D** Deep-seated landslide scar in Mount Buisaralao exposing bedrock geology of the hillslopes comprising predominantly of bedded siltstones and limestones. **E** Sigé river incising through landslide deposit forming steep debris bound terraces.

4.3 Deforestation, soil erosion and landslides

In mountainous regions, steep slope gradients and the availability of loose debris precondition these areas for landslides. Triggers are commonly prolonged or heavy rainfall, and earthquakes. These natural processes are an important factor for landscape evolution. However, if humans are exposed either deliberately or unintentionally to these processes, natural events turn to natural hazards with the potential to cause disasters. In East Timor, landslides occur regularly and cause considerable damage. Shallow earthquakes in the westernmost end of the country in the district of Bobonaro trigger landslides in the recent Synorogenic Megasequence (Viqueque formation) and the clay-rich lithologies of the Synorogenic Melange (Figure 4.17).
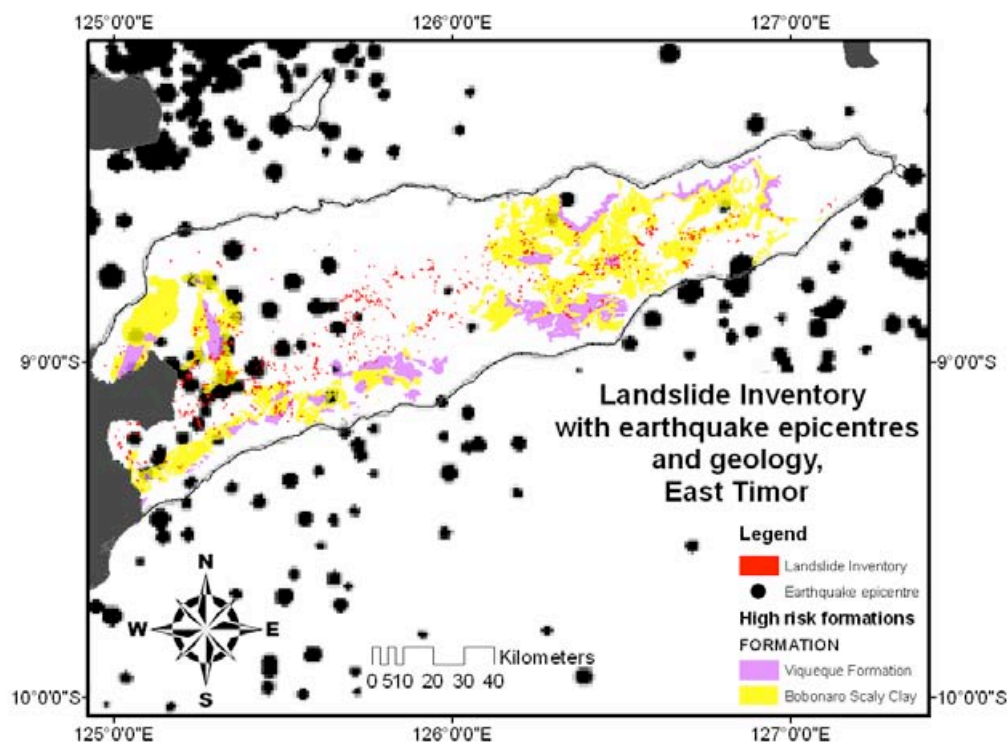

Figure 4.17: Landslide inventory high risk geological formations and earthquake epicentres taken from the ANSS catalogue. The westernmost end of East Timor experiences more shallow earthquakes. Many landslides in this region occur in the friable, unconsolidated Viqueque formation and Bobonaro Scaly Clay and are triggered by these shallow earthquakes. The Viqueque-Baucau area in the eastern end also has a large number of landslides occurring in the same unconsolidated lithologies but shallow earthquakes are uncommon.

Topography influences the weathering, depth, erodibility, infiltration and leaching of a soil. Bierenbroodspot (1986) classified land with slopes between 17º and 30º to be best used for grazing, as soil erosion cannot be controlled under permanent or shifting cultivation, and with slopes over 30º as unsuitable for sustainable cultivation and possibly requiring reforestation or crops providing perennial plant cover. In many parts of East Timor, relatively steep hillslopes are cultivated (Sandlund et al., 2001). Removal of vegetation on these steep upland hillsides unsuitable for agriculture

causes soil erosion both as surface erosion and as landslides (Figure 4.18). Slash-and-burn agriculture is widely practiced in many areas in Timor, including hilly country with steep slopes. Intensification of this system with reduced fallow periods due to increased population density has lead to the increased problems with soil erosion, higher frequency of more serious landslides destroying agriculture and forest areas, property and infrastructure (Sandlund et al., 2001).
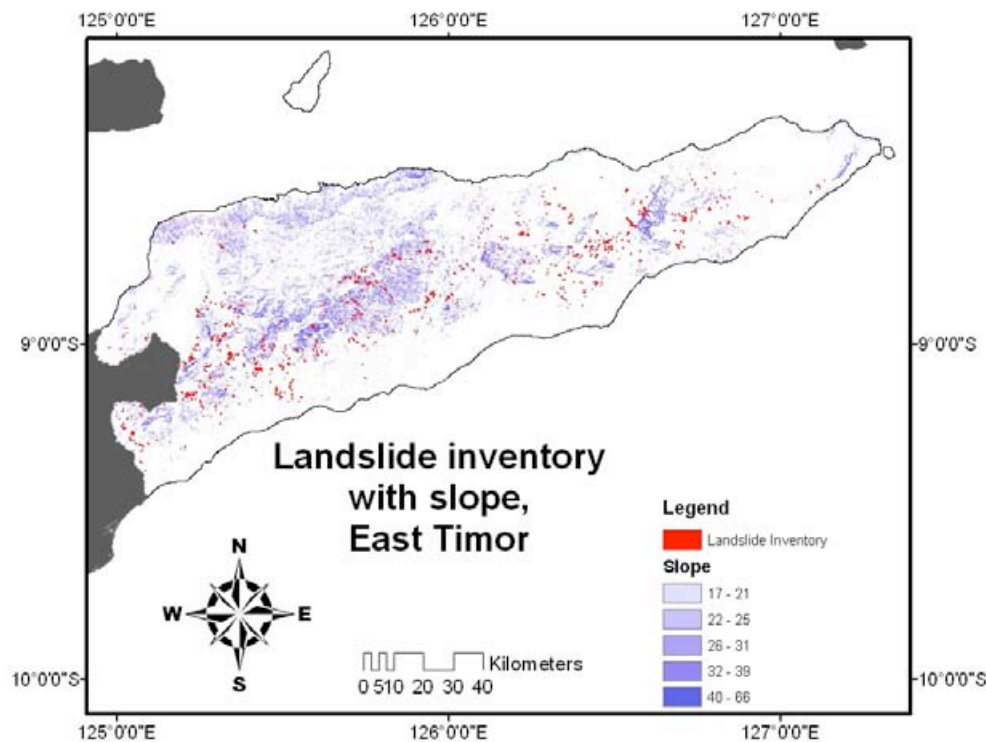

Figure 4.18: Landslide inventory showing areas with slopes greater than 17°. A majority of landslides are shown to be concentrated along the steep central mountain belt where slopes that generally exceed 40°.

Slope stability is influenced by climate, in particular the amount of water within the slopes, which is indirectly a function of precipitation and drainage conditions. Soil infiltration capacity governs the input of precipitation into the soil and increased rainfall intensities in excess of the infiltration capacity will result in a loss of water to the slope by overland flow (Crozier, 2010). Temperature is an important factor in affecting tropical soil fertility and structure (Mohr et al 1972). At temperatures below 20ºC humus is allowed to accumulate enriching the soil. At temperatures above 20ºC, humus is decomposed more quickly than it is formed, and soil fertility remains low. An important aspect of rainfall pattern is the fact that much rain comes in torrential downpours. In Dili, nearly 30% of annual mean rainfall may fall in one day. Hard torrential rain causes a high degree of surface runoff, and increased risk of soil erosion. In East Timor, the combination of steep terrain and torrential rains may cause disastrous erosion or landslides, in particular when natural vegetation has been removed. Seasonal monsoon rains falling on steep slopes cause frequent flash flooding and landslides, which regularly damage and destroy infrastructure, especially in rural areas. These events cause major disruption to the fragile road network of the

country, isolating communities and even districts for days, weeks, or even months. Widespread social, infrastructure, health and food vulnerabilities in Timor-Leste are further exacerbated by hazard and climate risks, lack of capacity and weak governance arrangements at the operating level. East Timor can be divided into six climatic zones based on rainfall and altitude, which serves as a proxy for temperature change with average temperatures decreasing with increasing altitudes (Figure 4.19) (For further discussion on the different zones, see Keefer, 2000).

In East Timor there are three broad landslide zones that can be characterised according to geology, slope, climate, and earthquakes (Figure 4.20-4.23).
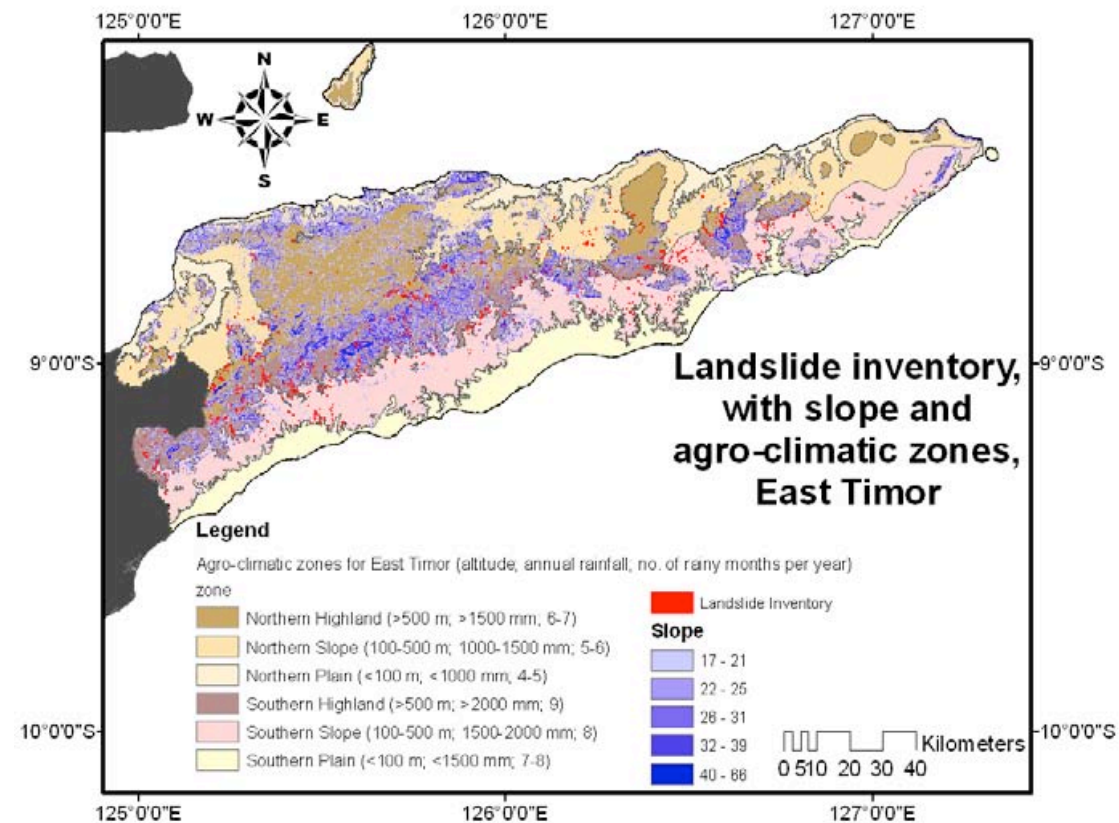
Figure 4.19: Landslide inventory showing slopes >17° and agro-climatic zones (ARPAPET, 1996). Landslides occur along the central axis of the mountain belt in the northern and southern highlands where annual rainfall can exceed 2000 mm and the wet season lasts for 9 months. Slopes in this region are generally greater than 40° and are cultivated.
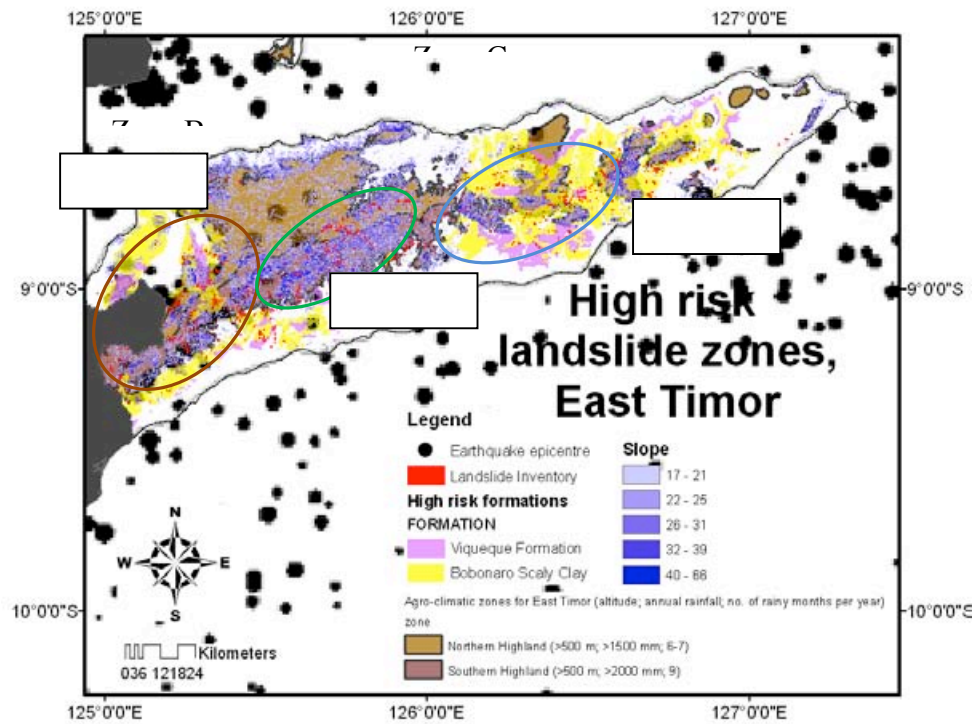
Figure 4.20: Landslide inventory showing slopes >17°, high risk geology formations, and agro-climatic zones in East Timor. Three broad landslide zones are identified in this study.
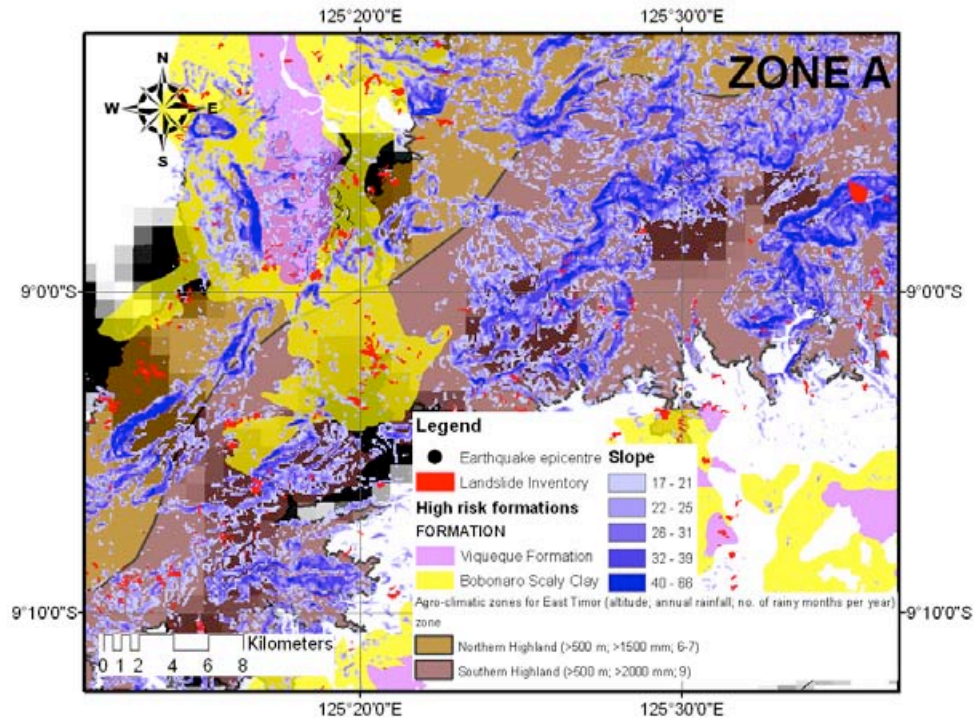
Figure 4.21: Zone A is characterised by frequent shallow earthquakes which trigger landslides in steep (>40º) cultivated slopes, and in clay-rich and unconsolidated lithologies in the highlands where annual precipitation exceeds 2000 mm
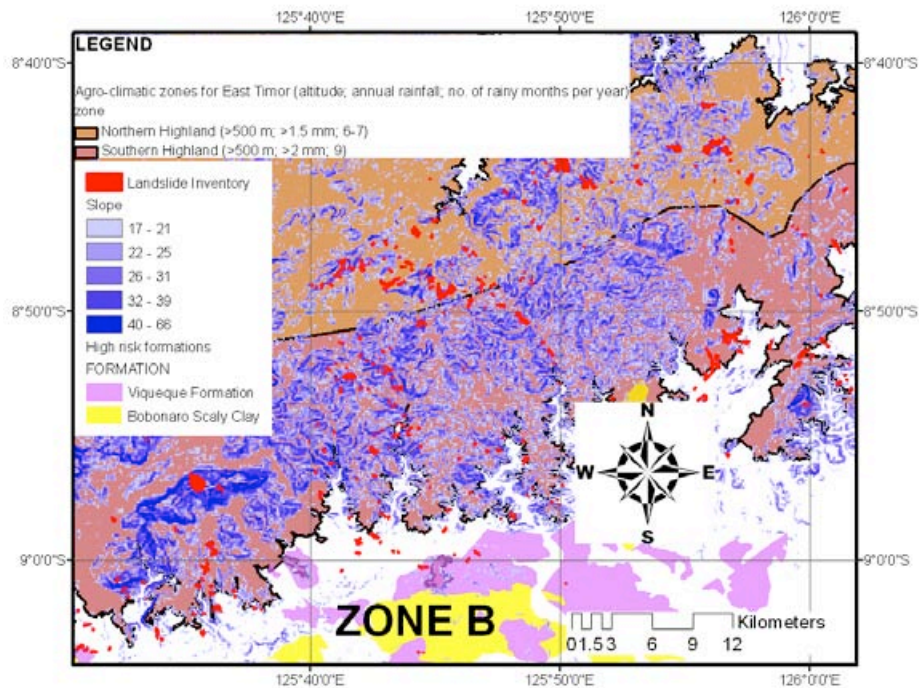
Figure 4.22: The central mountain Zone B is characterised by steep slopes, generally over 40°, where landslides are triggered by high precipitation events on the unstable slopes of cultivated highlands.
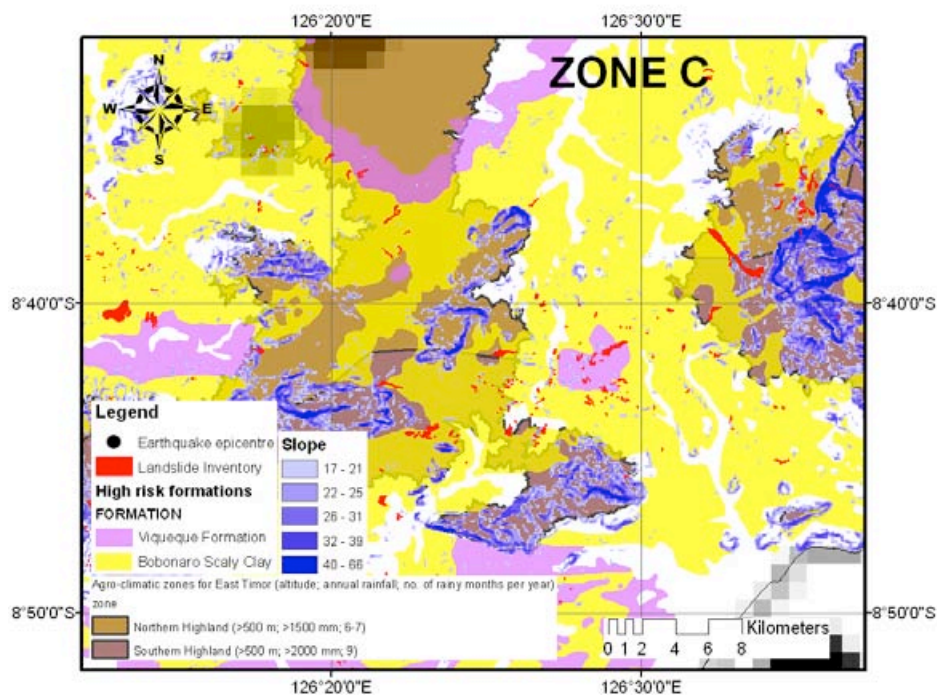
Figure 4.23: In Zone C, geology and climate are the dominant controls on landslides, rather than steep slopes. Here precipitation can reach 680 mm/month and landslides are clustered in the clay-rich lithologies of the Bobonaro Scaly Clay and the unconsolidated recent Viqueque formation.

27

4.4 Case Study: Lacalio landslide

4.4.1 Location of the field area

A large landslide occurred in the wet season of May 2010 near the village of Lacalio in the Quelicai sub-district of Baucau and is the focus of this case study (Figure 4.24). Quelicai is mountainous with steep, vegetated slopes at elevations in excess of 800m ASL and during the wet season can experience continuous days of heavy rainfall (Rodrigues et al., 2003). The catchment feeds three main rivers with mouths along the north coast of East Timor at Seical, Teknomata and Laga. Previous geological work has mapped the area as comprising of the Bobonaro Scaly Clay (Haig et al. 2007), and the Barique Formation, predominantly composed of basic tuffs (Audley-Charles, 1968). The area is prone to large and catastrophic landslides. Within 25 km^2 of the focus study area at least five separate landslips have occurred since 2001. The combined area of land affected by these slides is over 1 km^2 comprising a total of 4% of the land area.
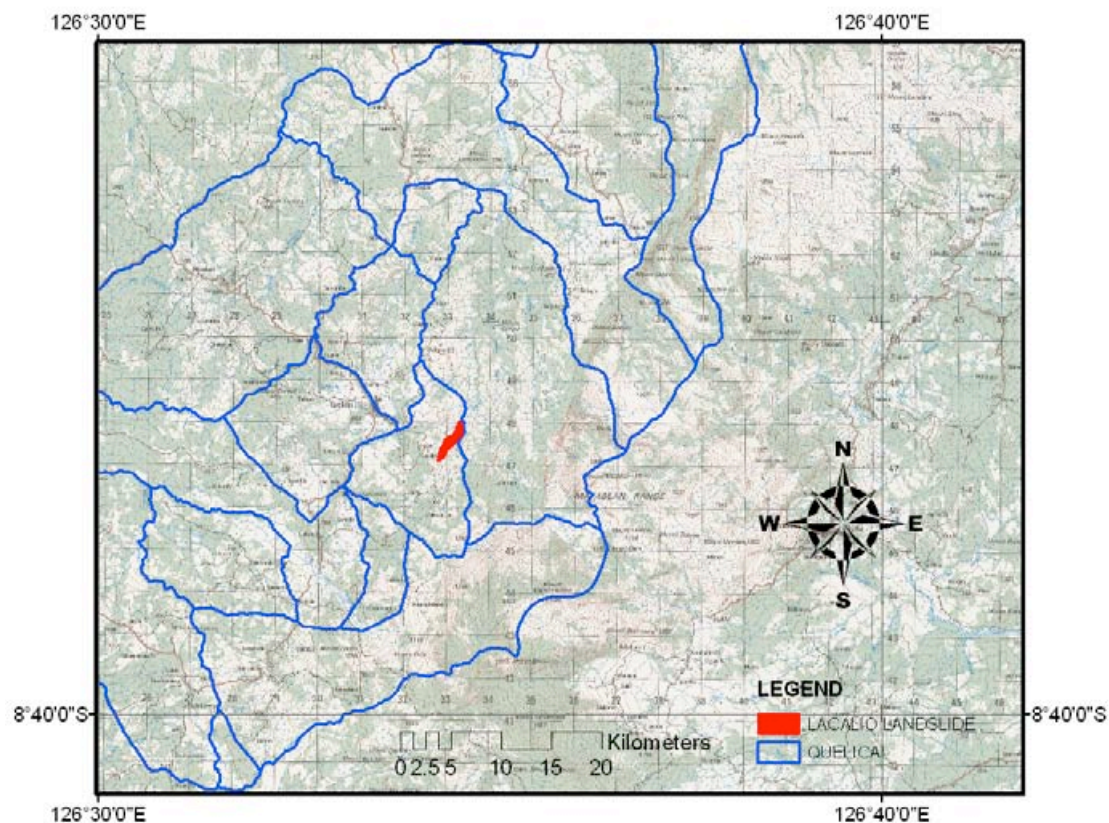
Figure 4.24: Locality map of Lacalio landslide located in the Quelicai sub-district near the village of Lacalio.

4.4.2 Lacalio landslide

Fieldwork undertaken during June/July 2010 field season investigated the recent May Lacalio landslide (Figure 4.25). The landslide appears to have been triggered by the preceding days of high precipitation with the majority of movement occurring over two days. The landslide flowed in a north-east direction and covered an area of 0.2

km^2. The area affected by the landslide had previously been used for subsistence agriculture. The steep hill slope had terraces cut into it to cultivate rice paddies and had been subject to annual burning to reduce excess plant material and control disease, pests and weeds. The adjacent hill slope has dense vegetation that, according to local inhabitants, has been relatively unchanged for at least 70 years. Studies of this landslide can give unique and important insights into possible underlying causes of landslides in the district, in particular, highlighting any lithologic and/or structural controls that could influence where the slides occur.

Figure 4.25: Image of Lacalio landslide and exposed scarp facing west, scarp length 180m.

4.4.3 Landslide dynamics

The landslide appears to have been deep seated extending below the soil and colluvial layers into the competent bedrock. The colluvium consists of a mixture of fine particles of mud and bedrock clasts ranging in size from sand to a maximum clast size approximately 20m by 20m (Figure 4.32).
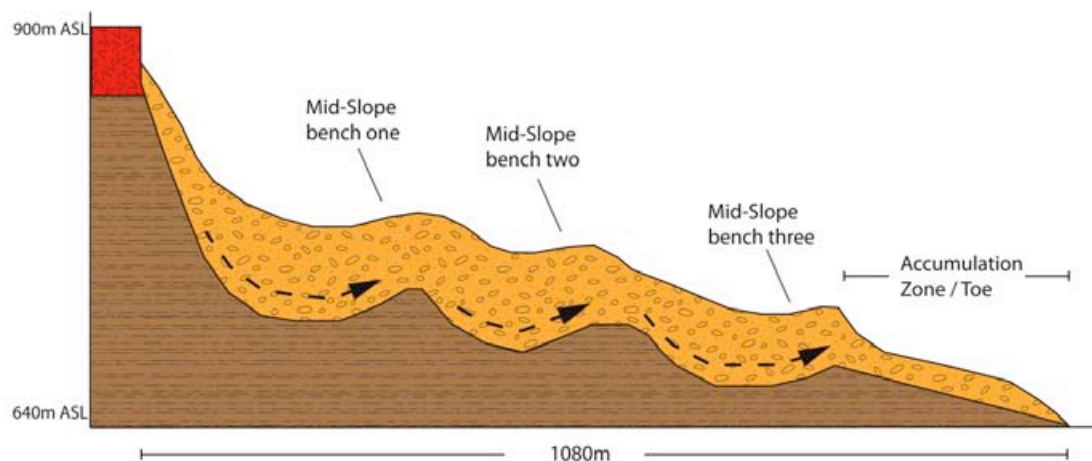
Figure 4.26: Schematic view of the profile of the Lacalio landslide. The profile shows the surface morphology of the landslide material (orange) and the likely contacts with the underlying mudstone (brown) and volcaniclastics (red). Geometrically the side has at least three mid slope benches with segments tilting back towards the headscarp as the blocks rotate around axes.

The internal structure of the landslide shows steep debris flows near the head of the slide followed by large translocational/rotational blocks (Figure 4.26). The surface of

rupture, glide plane, of this type of slide is curved concavely upward about an axis, which lies sub-parallel to the ground surface across the landslide. The effect of this rotation can be seen in profile of the geometry of the slide. The rotated blocks create a series of backwards tilting midslope benches and internal scarps. The distal end of the slide colluvium sits in a large accumulation zone or toe. Some areas within the landslide have remained relatively intact with some vegetation near to growth position. The landslide concentrates and channels precipitation and has created large areas of alluvium deposits and sag ponds. The channelling of the water has created a new stream system down the northwest side of the slide and has diverted a separate river along the east side (Figure 4.27). These drainage systems transport sediment from the landslide into the local river systems.

Figure 4.27: Image of the toe of the landslide facing northeast. Showing the last of the mid slope benches with a backwards tilt of 10º south followed by a large scarp. Areas of large alluvial deposits with a newly formed stream can be seen in the left corner of the image. Upright vegetation also with backwards tilt essentially 'surfed' the slide. Note people at scarp edge for scale.

4.4.4 Surrounding lithology and structure

Scarps along the western side of the slide exposed the underlying bedrock and structure to consist of a series of weak mudstones/shales overlain by weathered volcanics and volcaniclastics (Figure 4.28). Collection of field data in the surrounding area revealed the mudstone to be strongly bedded dipping towards the N/NE (Figure 4.29).

The cross section also reveals a possible deposit from a previous landslide on the same area, comprising angular clasts in a mud matrix. The contact between the colluviums deposit and the underlying mudstone bedrock (Figure 4.28) indicates that the previous slide also had a rotational component.

30

W

E

MUDSTONE

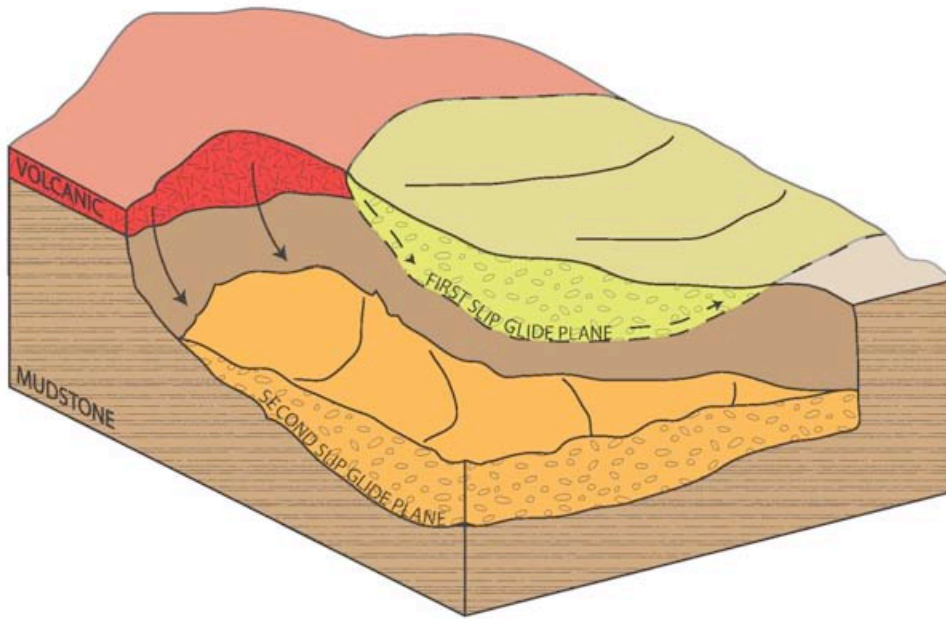**Figure 4.28:** Block diagram representing multiple slips. The scarp exposed by the second slip shows a series of bedded mudstone overlain by the volcaniclastics. The scarp also exposes a colluvium deposit most likely created by an earlier slide. The glide plane between the first slip and underlying mudstone is visible.

Figure 4.29: Bedded mudstone bedrock, the main component of the landslide colluvium.

Jointing (Figure 4.30) and faults along the scarp of the volcaniclastics indicates that the area has undergone previous deformation. The volcanic bedrock appears to have preferentially separated along one of the previous fault planes along the west side of the head scarp (Figure 4.31). Kinematically the movement on the fault plane is predominantly dextral strike slip with a minor normal component determined by the striations and slickenslides on the exposed surface. The movement on this fault is in opposition to the movement on the more recent landslip dismissing the possibility that these markings are related.

Figure 4.30 A & B: Jointing in the volcaniclastic bedrock in the headscarp. Note: yellow pencil for scale.
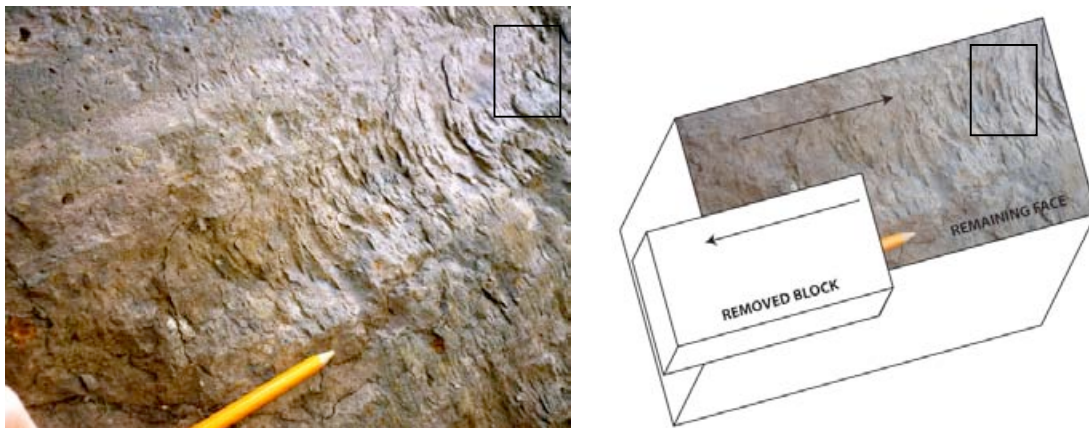
Figure 4.31: A Image, facing west, shows dextral strike slip surface of the remaining block of volcaniclastic bedrock in the headscarp orientation of striations and slikenslides visible. **B** Block diagram showing fault kinematics; strike 007/dip 72ºE.

Calcium carbonate deposits were found coating some of the large volcaniclastic clasts in the slide (Figure 4.32). Precipitation of this material suggests that prior to the landslide, fractures or cave like features existed in the bedrock allowing percolation of water. The presence of these features is likely to have also influenced the location at which the bedrock preferentially separated during the slide.

Figure 4.32: Largest volcaniclastic clast in the landslide material (20 m x 20 m) with calcium carbonate.

4.4.5 Continued monitoring and potential risk in the area

The areas immediately adjacent to the scarp show evidence for the beginnings of slippage in the top soil layers. Scarps from a few centimetres up to 1 m displacement are present in the surrounding areas. The largest scarp at 1 m is located in cleared land 160 m south of the main head scarp and a 70 cm displacement can be seen close by at 100 m south of head scarp. Both of these slips occurred approximately one month after the main slide according to local information. These displacements may be indication that the area is still a potential risk site for another large scale earth movement.

The scarp of greatest concern is located approximately 280 m north west from the landslide and offsets the regolith layer by 45 cm (Figure 4.33). The scarp strikes 350° and dips 72º towards the east. An outcrop near the scarp shows the bedrock under the regolith layer to consist of the same weak mudstones found in the bulk of the landslide. If this scarp is an early indicator of a mass movement event it has the potential to be devastating due to its close proximity to the village of Lacalio. The village consisting of many personal dwellings is located less then 20 m away on the slope directly below.

Figure 4.33: Top soil scarp, 45 cm, upslope from the village of Lacalio. Scarp appeared during the same heavy precipitation that occurred in May 2010, which triggered the Lacalio landslide. Photos taken by M. Quigley (2010).

Further evidence of creep and continued slippage over time can be seen in the surrounding area. In 2005 a landslip, located approximately 500 metres to the west of the more recent slide, affected an area of 0.01 km^2. New growth vegetation in the area of the landslide indicates that there have been continued periods of slip or creep post slide (Figure 4.34). Trees planted immediately following the 2005 slide now have a distinctive backwards tilt into the slope whilst younger vegetation, a year or so old, are orientated vertically. This suggests that movement has continued on the slope post 2005 but may have slowed or stopped from as a late as 2009.

The field program in this area aims to monitor the continued activity on the slide and in the surrounding area. Seven positional stakes have been placed and their geographical position recorded across the middle of the slide so that any change in their location due to further slips or creeps can be detected. As at October 2010, no further movements had occurred. Similarly, stakes have been position on opposite sides of many scarps in the surrounding area to help detect and quantify movement in these areas.

Figure 4.34 A & B: Older trees tilting back into the slope due to creep of soil during their growth.

4.4.6 Conclusion

The Lacalio landslide caused a great amount of damage in the local area. The destruction of crops and property has left the village with limitations on agriculture and has increased the need to take large detours. The geometry of the landslide surface indicates that the slide was a rotational slide with bedrock involvement. Exposure of the west scarp of the slide suggests that this area has been subjected to this type of rotational slide at least once in the past. Factors that contributed to the occurrence of this slide are the heavy days of precipitation preceding the slide, the mudstone bedrock with bedding dipping with the slope and structural features, such as faults, weakening bedrock. Evidence of continued creep and scarp production on surrounding hill slopes, combined with multiple accounts of previous landslides, strongly suggests that this area is at high risk of further landslides especially during periods of heavy precipitation.

35

5 Synthesis

The landscape of East Timor reflects a pre-steady-state topography, where there is an imbalance between uplift and denudational processes that redistribute mass across the Earth's surface. Topographic evolution of an active mountain belt at different stages of the sequence from catchment initiation up to entrenchment is observable over the region, and provides an excellent opportunity to evaluate landslides as a formative process i.e. their control on the geometry and denudation of a landscape.

A landslide inventory of 2005 in East Timor compiled during this study has been demonstrated to show a negative power law relation between number and landslide area over two orders of magnitude ($\sim 10^2 - 10^0$ km^2) for areas greater than 2.5 x 10^{-2} km^2. This relation reflects a scale invariance of the total area affected of landslide, including the zone of deposition. The slope of the power law implies that the bulk of the erosional work is done by infrequent high-magnitude events. The highest spatial density of landslides was observed in areas with clay-rich units of the Synorogenic Melange and soft recent material of the Synorogenic Megasequence. These terrains exhibit distinct denudation landforms, with lithology and climate acting as the primary controls for landsliding, rather than fluvial incision and the development of critical hillslopes. Landslides in East Timor also occur in areas with high slopes (>40˚) in the central northern and southern highlands. Here unsustainable agricultural practices on steep slopes and torrential rains cause soil erosion and landslides.

A large landslide, named the Lacalio landslide in this study, in the Quelicai sub-district occurred during the recent wet season in May and appears to have been triggered by several days of high-intensity precipitation. The landslide flowed in a north-east direction and covered an area of 0.2 km^2. The majority of movement occurred over two days and destroyed rice paddies, houses and gardens. The landslide appears to have been deep seated extending below the soil and colluvial layers into the competent bedrock. The bedrock comprises a series of weak mudstones overlain by weathered volcanic and volcanic sands. The volcanic bedrock appears to have preferentially separated along previous fault planes.

The internal structure of the landslide shows steep debris flows near the head of the slide followed by large translocational/rotational blocks. These blocks have created a series of midslope benches with backward tilting and internal scarps. Some areas within the landslide have remained relatively intact with some vegetation near to growth position. Large alluvial areas and sag ponds are present due to large amounts of drainage across the site. These drainage systems transport sediment from the new landslide into the local river systems.

This study extends the findings of Hovius et al. (1998) and Strasser & Schlunegger (2005), drawing the same conclusions: primarily that the steady-state morphology of a mountain belt is intimately related to its initial phase of growth. The emergence of an orogen is generally characterized by an early phase of rapid surface uplift and the concomitant evolution of montane topography, leading in some cases to a steady state in which tectonic mass flux is balanced by erosion. This early phase of mountain growth is exemplified throughout East Timor. These observations follow Hovius et al.'s (1997) conclusions that the steady state morphology of a mountain belt

ultimately derives from the organization of surface processes during preceding formative phase of mountain growth, in which landsliding is probably the critical rate limiting process.

Geomorphic hazards, such as landslides, can be regarded as the group of threats to human resources resulting from the instability of Earth's surfaces features. Magnitude and frequency, as well as temporal and spatial scale, are key geomorphic concepts strongly correlated to natural hazards. Wolman and Miller (1960) introduced the importance of magnitude and frequency of different events and their significance on the landscape as a result of the total work performed by them. Therefore, the importance of both extreme events and high-frequency, low-magnitude events within geomorphic processes is determined by the relation of the work done on the landscape to the particular landforms resulting from it. These concepts are essential for the assessment of natural hazards as the dynamism of the Earth's surface is enclosed within a temporal and spatial scale. The response of the landform to the changes caused by the processes corresponds to the magnitude and frequency of the events, the resistance of the involved materials and the size of the concerned landform (Summerfield, 1991).

In order to cope with the consequences of natural hazards and their interaction with people living in mountainous areas prone to landsliding, geomorphology is an essential part to undertake risk assessment based on geomorphic hazard and risk zonation. Natural hazards cannot be prevented, but the understanding of the process and scientific methodologies to predict patterns of behaviour of such processes can be powerful tools to help reduce natural vulnerability. Geomorphology studies can provide theoretical and applied approaches to the prevention of natural disasters, such as landslides, in terms of origin and dynamism of the physical processes. Furthermore, geomorphologists could also offer important contributions based on the understanding of the interaction between natural hazards (natural vulnerability) and the societies (human vulnerability). Geomorphologists assist in the reduction of natural vulnerability in three different ways (Alcantara-Ayala, 2002):

- Firstly, by enriching the theoretical knowledge of geomorphology, in this case landslide geomorphology, which is the base of the application of our discipline;

- Developing prediction models for different processes, such as landsliding;

- Through diversified approaches of applied geomorphology for the prevention of natural disasters.

References

1. Alcantara-Ayala, I., 2002. Geomorphology, natural hazards, vulnerability and prevention of natural disasters in developing countries. *Geomorphology*, **47**, 197-124.

2. ANSS Earthquake Catalogue, access June 17, 2010: http://www.ncedc.org/cnss/catalog-search.html

3. ARPAPET, 1996. Agro-climatic Zones of East Timor. Lindsay Evans April, 1996. Kantor Wilyah dep. Pertanian Prop. Tim – Tim. Jln Estrada de Balide, Dili, Tim – Timor 88112, Indonesia.

4. Audley-Charles, M. G., 1968. The geology of Portuguese Timor. *Memoirs of the Geological Society of London*, **4**, 1-75.

5. Audley-Charles, M. G., 2004. Ocean trench blocked and obliterated by Banda forearc collision with Australian proximal continental slope. *Tectonophysics*, **389** (1-2), 65-79.

6. Bierenbroodspot, J., 1986. Soil erosion and its control in West Timor. NTT integrated area development project. ACIL Australia Pty. Ltd.

7. Brardinoni, F., Church, M., 2004. Representing the landslide magnitude-frequency relation: Capilano River Basin, British Columbia. *Earth Surface Processes and Landforms*, **29**, 115-124.

8. Brardinoni, F., Slaymaker, O., Hassan, M. A., 2003. Landslide inventory in a rugged forested watershed: a comparison between air-photo and field survey data. *Geomorphology*, **54**, 179-196.

9. Buccolini, M., Coco, L., 2010. The role of the hillside in determining the morphometric characteristics of "calanchi": The example of Adriatic central Italy. *Geomorphology*, **123**, 200-210.

10. Carter, D. J., Audley-Charles, M. G., Barber, A. J., 1976. Stratigraphical analysis of island arc-continental margin collision in eastern Indonesia. *Journal of the Geological Society*, **132**, 179-198.

11. Crozier, M. J., 2010. Deciphering the effect of climate change on landslide activity: A review. *Geomorphology*, **124**, 260-67.

12. Dadson, S. J., Hovius, N., Chen, H., Dade, W. B., Hsieh, M. L., Willett, S. D., Hu, J. C., Horng, M. J., Chen, M. C., Stark, C. P., Lague, D., Lin, J. C., 2003. Links between erosion, runoff variability and seismicity in the Taiwan orogen. *Nature*, **426**, 648-651.

13. Dai, F. C., Lee, C. F., 2001. Frequency-volume reaction and prediction of rainfall-induced landslides. *Engineering Geology*, **59**, 253-266.

14. Durand, F., 2006. East Timor, a country at the crossroads of Asia and the Pacific, a geo-historical Atlas. Silkworm Books, 198pp.

15. Government of Timor-Leste, 2008. National Disaster Risk Management Policy. NDMD.

16. Government of Timor-Leste, 2007. IV Constitutional Government Program of the Council of Ministers 2007-2012.

17. Guthrie, R. H., Evans, S. G., 2007. Work, persistence, and formative events: the geomorphic impact of landslides. *Geomorphology*, **88**, 266-275.

18. Guzzetti, F., Malamud, B. D., Turcotte, D. L., Reichenbach, P., 2002. Power-law correlations of landslide areas in central Italy. *Earth and Planetary Science Letters*, **195**, 169-183.

19. Haig, D. W., McCartain, E. W., 2007. Carbonate pelagites in the post-Gondwana succession (Cretaceous – Neogene) of East Timor. *Australian Journal of Earth Sciences*, **54** (6), 875-897.

20. Haig, D. W., McCartain, E. W., Barber, L., Backhouse, J., 2007. Triassic – lower Jurassic foraminiferal indices for Bahaman-type carbonate-bank limestones, Cablac Mountain, East Timor. *Journal of Foraminiferal Research*, **37** (3), 248-264.

21. Hall, R., Wilson, M. E. J., 2000. Neogene sutures in eastern Indonesia. *Journal of Asian Earth Sciences*, **18** (6), 781-808.

22. Harris, R. A., Hurford, A., Carter, A., 2000. Thermal history of Australian passive margin cover sequences accreted to Timor during Late Neogene arc-continent collision, Indonesia. *Journal of Asian Earth Sciences*, **18** (1), 47-69.

23. Hovius, N., Stark, C. P., Allen, P. A., 1997. Sediment flux from a mountain belt derived by landslide mapping. *Geology*, **25** (3), 231-234.

24. Hovius, N., Stark, C. P., Hao-Tsu, C., Jiun-Chuan, L., 2000. Supply and removal of sediment in a landslide-dominated mountain belt: Central Range, Taiwan, *The Journal of Geology*, **108**, 73-89.

25. Hovius, N., Stark, C. P., Tutton, M. A., Abbott, L. D., 1998. Landslide-driven drainage network evolution in a pre-steady-state mountain belt: Finisterre Mountains, Papua New Guinea. *Geology*, **26** (12), 1071-1074.

26. Hungr, O., Evans, S. G., Hazzard, J., 1999. Magnitude and frequency of rock falls and rock slides along the main transportation corridors of southwestern British Columbia. *Canadian Geotechnical Journal*, **36**, 224-238.

27. Keefer, G., 2000. Report on the Restoration of Meteorological Network—Timor Loro'Sae. Report II, United Nations Transitional Administration in East Timor, Dili, East Timor, 44 pp.

28. Keep, M., Haig, D. W., 2010. Deformation and exhumation in Timor: distinct stages of a young orogeny. *Tectonophysics*, **483**, 93-111.

29. Malamud, B. D., Turcotte, D. L., Guzzetti, F., Reichenbach, P., 2004. Landslide inventories and their statistical properties. *Earth Surface Process Landforms*, **29**, 657-684.

30. McCartain, E., Backhouse, J., Haig, D., Balme, B., Keep, M., 2006. Gondwana-related Late Permian palynoflora foraminifers and lithofacies from the Wailuli Valley, Timor Leste. *Neues Jahrbuch fūr Geologie und Paläontologie, Abhandlungen*, **240**, 53-80.

31. Mohr, E. C. J., van Baren, F. A., van Schuylenborgh, J., 1972. Tropical soils: a comprehensive study of their genesis. Mouton, The Hague, 481 pp.

32. Monk, K. A., de Fretes, Y., Reksodiharjo-Lilley (eds.), 1997. The ecology of Nusa Tenggara and Maluku. *The ecology of Indonesia in Series*, **V**, Oxford University Press.

33. Pelletier, J. D., Malamud, B. D., Blodgett, T., Turcotte, D. L., 1997. Scale-invariance of soil moisture variability and its implications for the frequency-size distribution of landslides. *Engineering Geology*, **48**, 255-268.

34. Rodrigues, D., Ayala-Carcedo, F. J., Brilha, J., Tavares, A., Nogueira, P., 2003. Landslides in the Baucau and Viqueque districts of East Timor. *Landslide News*, **14-15**, 36-38.

35. Sandlund, O., I. Bryceson, D. Carvalho, N. Rio, J. Silva, and M. Silva. 2001. Assessing Environmental Needs and Priorities in East Timor: Final Report. UNDP and Norwegian Institute for Nature Research NIÑA, Trondheim, Norway. 46. pp.

36. Strasser, M., Schlunegger, F., 2005. Erosional processes, topographic length-scales and geomorphic evolution in arid climatic environments: the 'Lluta collapse', northern Chile. *International Journal of Earth Sciences*, **94**, 433-446.

37. Summerfield, M. A., 1991. Global Geomorphology: An Introduction to the Study of Landforms. Wiley, New York, 537 pp.

38. UNISDR. 2007. Hyogo Framework for Action 2005-2015: Building the Resilience of Nations and Communities to Disasters.

39. Universidade Técnica de Lisboa, Faculdade de Arquitectura, 2002. Atlas de Timor Leste. LIDEL, Ediçôes Técnicas, Lisboa. 169 p.

40. Wolman, M. G., Miller, J. P., 1960. Magnitude and frequency of forces in geomorphic processes. *Journal of Geology*, **69** (1), 54-74.

41. World Bank. 2010. Timor-Leste Country Assessment: Reducing the Risk of Disasters and Climate Variability in the Pacific Islands.